Bone 120 (2019) 371–386

Contents lists available at ScienceDirect

Bone

journal homepage: www.elsevier.com/locate/bone

Full Length Article

miRNA-seq analysis of human vertebrae provides insight into the mechanism underlying GIOP

Hui Ren[a,c,1], Xiang Yu[b,c,1], Gengyang Shen[b,c,1], Zhida Zhang[b,c], Qi Shang[b,c], Wenhua Zhao[b,c], Jinjing Huang[b,c], Peiyuan Yu[b,c], Meiqi Zhan[b,c], Yongqiang Lu[b,c], Ziyang Liang[b,c], Jingjing Tang[a,c], De Liang[a,c], Zhensong Yao[a], Zhidong Yang[a], Xiaobing Jiang[a,c,*]

[a] Department of Spinal Surgery, The First Affiliated Hospital of Guangzhou University of Chinese Medicine, Guangzhou 510405, China
[b] First Clinical Medical College, Guangzhou University of Chinese medicine, Guangzhou, China, 510405
[c] Lingnan Medical Research Center, Guangzhou University of Chinese Medicine, Guangzhou 510405, China

ARTICLE INFO

Keywords:
Glucocorticoid-induced osteoporosis
miRNA
High throughput sequencing
Vertebrae
Human

ABSTRACT

High-throughput sequencing (HTS) was recently applied to detect microRNA (miRNA) regulation in age-related osteoporosis. However, miRNA regulation has not been reported in glucocorticoid-induced osteoporosis (GIOP) patients and the mechanism of GIOP remains elusive. To comprehensively analyze the role of miRNA regulation in GIOP based on human vertebrae and to explore the molecular mechanism, a high-throughput sequencing strategy was employed to identify miRNAs involved in GIOP. Twenty-six patients undergoing spinal surgery were included in this study. Six vertebral samples were selected for miRNA sequencing (miRNA-seq) analysis and 26 vertebral samples were verified by qRT-PCR. Bioinformatics was utilized for target prediction, to investigate the regulation of miRNA-mRNA networks, and Gene Ontology (GO) and Kyoto Encyclopedia of Genes and Genomes (KEGG) pathway analyses. Six significantly up-regulated miRNAs (including one novel miRNA) and three significantly down-regulated miRNAs were verified via miRNA-seq and verified in the vertebrae of GIOP patients. Up-regulated miRNAs included hsa-miR-214-5p, hsa-miR-10b-5p, hsa-miR-21-5p, hsa-miR-451a, hsa-miR-186-5p, and hsa-miR-novel-chr3_49,413 while down-regulated miRNAs included hsa-let-7f-5p, hsa-let-7a-5p, and hsa-miR-27a-3p. Bioinformatics analysis revealed 5983 and 23,463 predicted targets in the up-regulated and down-regulated miRNAs respectively, using the miRanda, miRBase and TargetScan databases. The target genes of these significantly altered miRNAs were enriched to 1939 GO terms and 84 KEGG pathways. GO terms revealed that up-regulated targets were most enriched in actin filament-based processes (BP), anchoring junction (CC), and cytoskeletal protein binding (MF). Conversely, the down-regulated targets were mostly enriched in multicellular organismal development (BP), intracellular membrane-bounded organelles (CC), and protein binding (MF). Top-10 pathway analysis revealed that the differentially expressed miRNAs in GIOP were closely related to bone metabolism-related pathways such as FoxO, PI3K-Akt, MAPK and Notch signaling pathway. These results suggest that significantly altered miRNAs may play an important role in GIOP by targeting mRNA and regulating biological processes and bone metabolism-related pathways such as MAPK, FoxO, PI3K-Akt and Notch signaling, which provides novel insight into the mechanism of GIOP and lays a good foundation for the prevention and treatment of GIOP.

1. Introduction

Glucocorticoid-induced osteoporosis (GIOP) is a systemic bone disease induced by glucocorticoids (GCs). The incidence of GIOP continues to increase with the widespread use of GCs, and GIOP has been identified as the most common type of secondary osteoporosis [1]. Emerging evidence has demonstrated that bone fragility induced by GIOP is much more serious than that induced by postmenopausal osteoporosis, and GIOP has higher disability and mortality rates [2]. Excessive or prolonged GC treatment has been believed to play a major role in inhibiting bone formation [3,4]. However, the underlying mechanism of GIOP has not yet been confirmed [5]. Thus, it is still an important and urgent project to find out how to research the mechanism and treatment of GIOP.

* Corresponding author at: Department of Spinal Surgery, The First Affiliated Hospital of Guangzhou University of Chinese Medicine, Guangzhou 510405, China.
E-mail address: spinedrjxb@sina.com (X. Jiang).
[1] The co-first authors.

https://doi.org/10.1016/j.bone.2018.11.013
Received 4 April 2018; Received in revised form 16 November 2018; Accepted 19 November 2018
Available online 29 November 2018

microRNAs (miRNAs) are a class of small non-coding RNA molecules approximately 19–25 nucleotides in length that regulate gene expression either by degrading target mRNAs or inhibiting gene translation [6–8]. miRNAs regulate genes by complementary binding of their seed sequence to the 3′-untranslated region of their target mRNAs [9,10]. An increasing number of studies have shown that miRNAs may become a new and attractive treatment target for osteoporosis or other bone diseases, even though some problems associated with potential off-target effects and the need for effective delivery methods in vivo remain unsolved [11]. Several miRNAs, such as miR-223 and miR-103a, regulate bone metabolism by modulating the differentiation and activity of osteoblasts and osteoclasts [12–14]. miRNAs promote bone formation by enhancing the bone morphogenic protein (BMP) and Wnt/β-catenin pathways, thus promoting the activity or expression of transcription factors such as Runx2 and SP7 [15–19]. Moreover, a few studies have confirmed that miRNAs play important roles in various stages of bone formation [14]. In terms of bone resorption regulation, miRNAs promote the phenotype of Dicer dysfunction in osteoclast differentiation and osteoclast cell lineage. Recently, several differentially expressed, such as miR106b, miR365, and miR199, have been found in a few GIOP studies [20–22], although they are limited to the animal or cellular level, and there could be some species differences in miRNA expression. Therefore, it is of great significance to explore the pathogenesis of GIOP, and seek an effective target for the prevention and treatment of GIOP base on microbiology.

High-throughput sequencing (HTS) technology, an important approach for screening mechanisms of diseases and drug interventions, has been widely used in many fields, including the whole genome, transcriptome, and regulatory noncoding RNAs (such as miRNAs, LncRNAs and CirRNAs). HTS has been combined with computational techniques to detect miRNA dynamics in mesenchymal stem cells (MSCs) and bone tissue of age-related osteoporosis [23]. Moreover, differentially expressed serum miRNAs serve as candidate biomarkers in patients with primary osteoporosis [24]. However, differential miRNA expression has not been reported in GIOP patients and the mechanism of GIOP remains elusive. In the present study, we aimed to identify differentially expressed miRNAs in GIOP vertebrae and the mechanism involved. We screened and verified the differentially expressed miRNAs by collecting GIOP vertebrae, and forecasted the target genes based on bioinformatics analysis. Furthermore, to better understand the biological processes (BP), cellular component (CC) and molecular functions (MF) of miRNAs, we performed clustering GO and pathway analyses according to target gene function to establish an experimental basis for a robust therapeutic target or diagnostic tool for precision medicine in GIOP.

2. Materials and methods

2.1. Ethics statement

The current study was approved by the Clinical Research Ethics Committee of the First Affiliated Hospital of Guangzhou University of Chinese Medicine (Guangzhou, People's Republic of China) with approval number ZYYECR[2016]028. Great care was taken to ensure that the patients were well-informed of the study protocol and any risks, and we never allowed the study procedures to compromise the wellbeing of any patient.

2.2. Sample preparation

Sample preparation occurred over two stages. Three GIOP patients and three control patients were included in the first (discovery) stage, while 26 patients (13 in the GIOP group, 13 in the control group) were included in the second (verification) stage. Twenty-six patients undergoing spinal surgery at the Spine Orthopedic of the first Affiliated Hospital of Guangzhou University of Chinese Medicine between 2016 and 2017 were included. GIOP patients were defined as those with a diagnosis of osteoporosis (defined as a T score of ≤ -2.5) and osteopenia (defined as a T score > -2.5 and < -1.0 when compared to young healthy in terms of bone mineral density [BMD] [25]) and long-term GC use (≥ 6 months), in accordance with literature standards [25,26]. Inclusion criteria were as follows: GIOP group, 1) Conforming to the diagnostic standard of osteoporosis, 2) Long-term GC use (≥ 6 months), 3) Fragile lumbar fractures (acute fracture, i.e., within 2 weeks), 4) Clear indication of vertebroplasty or internal fixation, 5) Agreed to undergo surgery, and 6) Agreed to take part in this study; Control group, 1) Underwent a spinal operation because of lumbar degenerative diseases (such as lumbar spondylolisthesis and lumbar spinal stenosis) and 2) No osteoporosis or other metabolism disease. Accordingly, the exclusion criteria were as follows: GIOP group, 1) Previous long-term use of GCs but withdrawn for > 1 year, 2) Complicated with other diseases causing osteoporosis, such as idiopathic osteoporosis, diabetes, hyperthyroidism, or tumor, 3) Female in menopause or postmenopausal, and 4) Receiving any anti-osteoporosis treatment (bisphosphonates, Forsteo, denosumab or other anti-osteoporotic drug); Control group, 1) History of GC use, 2) Osteoporosis or other bone metabolism disease, 3) Marasmus, anemia, malnutrition, long-term smoking and/or drinking, and 4) Female in menopause or

Table 1
Inclusion criteria and exclusion criteria of two groups.

Diagnosed standard of osteoporosis	Osteoporosis was diagnosed based on dual-energy X-ray absorptiometry: Osteoporosis defined as a T score of ≤ -2.5	
Inclusion criteria	GIOP group	1. Conforming to the diagnostic standard of osteoporosis; 2. Long-term GC use (≥ 6 months); 3. Fragile lumbar fractures (acute fracture, i.e., within 2 weeks); 4. Clear indication of vertebroplasty or internal fixation; 5. Agreed to undergo surgery; 6. Agreed to take part in this study.
	Control group	1. Underwent a spinal operation because of lumbar degenerative diseases (such as lumbar spondylolisthesis and lumbar spinal stenosis); 2. No osteoporosis or other metabolism disease.
Exclusion criteria	GIOP group	1. Previous long-term use of GCs but withdrawn for > 1 year; 2. Complicated with other diseases causing osteoporosis, such as idiopathic osteoporosis, diabetes, hyperthyroidism, or tumor; 3. Female in menopause or postmenopausal; 4. Receiving any anti-osteoporosis treatment (bisphosphonates, Forsteo, denosumab or other anti-osteoporotic drug)
	Control group	1. History of GC use; 2. Osteoporosis or other bone metabolism disease; 3. Marasmus, anemia, malnutrition, long-term smoking and/or drinking; 4. Female in menopause or postmenopausal.

postmenopausal. Inclusion and exclusion criteria are also listed in Table 1.

Data on age, gender, bone density (bone mineral content [BMC], BMD, T score), body mass index (BMI), and serum Ca, Mg, P, and alkaline phosphatase (ALP) were collected. Vertebral bone samples from both groups were collected via bone biopsy during the operation and stored at liquid nitrogen for HTS and quantitative real-time PCR (qRT-PCR) analysis. Before the operation, when the patient was under pedicle internal fixation or vertebroplasty, 1–2 long strips (two sides, approximately 40–60 mg/strip) removed from the vertebra using bone biopsy needle.

2.3. RNA extraction

Approximately 80 mg vertebral bone tissue was used to grind with liquid nitrogen condition sufficiently. Ultimately, bone powder were collected as much as possible and placed in a sterilized RNA-free tube, 1.2 ml TRIZOL was fully dissolved with powder bone sufficiently for approximately 10 mins. After sufficiently splitting decomposition, 200 μL chloroform was added, thorough mixing (no precipitated impurities), centrifuged at 12000 rpm at 4 °C 15 mins, the supernatant was collected and 200 μL isopropyl alcohol was added into the supernatant. Following, the RNA was isolated from the resulting extract using the TAKARA MiniBEST Universal RNA Extraction kit (Cat# 9767, Lot# AK1601) according to the manufactor's instructions. And contaminating genomic DNA (gDNA) was removed with RNase-free DNase I (Takara, Japan) according to the manufacturer's protocol. Total RNA integrity was assessed using a RNA NanoDrop ND-1000 spectrophotometer (NanoDrop Inc., Wilmington, DE, USA) for quality control. RNA integrity and genomic DNA contamination were evaluated by denaturing agarose gel electrophoresis and the intensities of 28 s, 18 s and 5 s ribosomal RNA bands were assessed.

2.4. miRNA sequencing library construction and HTS

Approximately 1 μg of RNA from each sample was used for the subsequent cDNA library construction following the protocol of the NEBNext® Multiplex Small RNA Library Prep Set for Illumina® (Set 2) (Kit: NEB #E7300; Illumina, San Diego, CA, USA). When the purity, concentration and the integrity of total RNAs were all up to standard, the total RNA of each sample was used to prepare the miRNA sequencing (miRNA-seq) library which included the following steps: 1) 3′-adaptor ligation; 2) 5′-adaptor ligation; 3) the cDNA synthesis was performed using Illumina real-time primers and amplification primers; 4) PCR amplification; and 5) size selection of 135–155 bp PCR-amplified fragments (corresponding to ~15–35 nt small RNAs). After the library was constructed, the quality and concentration of the sequencing library were assessed by Agilent 2100 Bioanalyzer using the Agilent DNA 1000 chip kit (Agilent, part # 5067-1504). Samples were diluted to a final concentration of 8 pM. The libraries were denatured as single-stranded DNA molecules, captured on Illumina flow cells, amplified in situ as clusters, and finally sequenced for 36 cycles on Illumina HiSeq 2000 platform according to the manufacturer's instructions. The TruSeq Rapid SR Cluster Kit (# GD-402-4001, Illumina) was used to cluster on Illumina cBot, and the cDNA libraries were sequenced by using a TruSeq Rapid SBS Kit (# fc-402-4002, Illumina) on the Illumina HiSeq 2000 platform (Illumina Inc., San Diego, California, USA) according to the manufacturer's protocol.

2.5. miRNA-seq data analysis

After sequencing, the Solexa CHASTITY quality-filtered reads were harvested as clean reads. The adaptor sequences were trimmed and the adaptor-trimmed-reads (≥15 nt) retained. miRDeep2 software was used to predict the novel miRNAs with these trimmed reads, which were then aligned to merged pre-miRNA databases (i.e., known pre-miRNA from miRBase v21 plus the newly predicted pre-miRNAs) using Novoalign software (ver.2.07.11 [http://www.novocraft.com/main/index.php]) with one mismatch at most. The number of mapped tags that was given by the raw expression levels of that particular miRNA. To correct for differences in tag count between samples, the tag counts were scaled to TPM (copy number of transcripts per million) based on the total number of aligned tags. When comparing the differentially expressed miRNA profiles between two groups, fold change and *P*-values were calculated and used to identify significant differentially expressed miRNAs.

Hierarchical clustering was utilized to display the differentially expressed miRNAs. miRNA target prediction was performed by using three database: miRanda database (http://www.microrna.org/microrna/home.do), Microcosm Targets Version 5 [formerly miRBase Targets] (http://www.ebi.ac.uk/enright-srv/microcosm/htdocs/targets/v5/) and Targetscan version 6.2 (http://www.targetscan.org/vert_60/). To improve prediction accuracy, the overlap of the predicted results from the three programs was considered to represent the final result of predicted target mRNAs (When the miRNAs of GIOP_vs_CON_down and GIOP _vs_CON_up were predicted as target genes, the values of 3 databases including MiRanda, miRbase and Targetscan were 2). Venn diagram showed the expression distribution of all the target genes of differentially expressed miRNAs. And then the GO and KEGG pathway analysis were performed based on the differentially expressed genes (DEGs).

2.6. GO and KEGG pathway analyses

The Gene Ontology project provides a controlled vocabulary to describe gene and gene product attributes in any organism (http://www.geneontology.org). The ontology covers three domains: Biological Process, Cellular Component and Molecular Function. Fisher's exact test is used to find if there is more overlap between the DE list and the GO annotation list than would be expected by chance. The *P*-value denotes the significance of GO terms enrichment in the DE genes. To further evaluate the potential functions of these miRNA target genes, we applied KEGG pathway analysis (http://www.genome.jp/). The network of miRNA target genes was shown in each pathway in the form of a pathway map. Pathway analysis is a functional analysis that maps genes to KEGG pathways. The *P*-value (EASE-score, Fisher's *P*-value or hypergeometric *P*-value) denotes the significance of the pathway correlated to the conditions. The lower the *P*-value, the more significant are the GO term and the pathway. The recommended *P*-value cut-off was 0.05.

2.7. Cytoscape network construction

To reveal correlations among miRNAs, miRNA target genes, and target genes in GIOP and miRNA-mRNA networks were constructed using the Cytoscape software manual (http://www.cytoscape.org) [27].

2.8. Novel miRNA prediction

Novel miRNAs were identified by miRDeep2 [28]. Based on a simple model of pre-miRNA processed by Dicer protein, miRDeep2 not only replicates most of the known miRNAs in heterogeneous and deeply sequenced samples, but also credibly predicts novel miRNAs.

2.9. Differential miRNA verification by qRT-PCR

qRT-PCR was carried out to validate the miRNAs identified by deep sequencing. We chose two significantly up-regulated and 12 significantly down-regulated miRNAs closely associated with bone metabolism or homeostasis. Another 11 miRNAs with a high fold change, high tag frequency and high reads in the original sequencing data, but no significant differences, were also chosen. In total, 25 miRNAs were

verified by qRT-PCR. In the second verification stage, the total RNA from vertebral samples of 26 patients was extracted according to Section 2.3 (see above). The samples were then reverse-transcribed into cDNA using the Mir-X™ miRNA First Strand Synthesis Kit (Code No. 638315; Takara, Tokyo, Japan) according to the manufacturer's instructions. cDNA was quantified by the Mir-X™ miRNA qRT-PCR SYBR® Kit (Code No. 638316, Takara) using a 25 μL reaction mixture that consisted of 2 μL diluted cDNA, 9 μL ddH_2O, 0.5 μ L ROX Dye (50×), 0.5 μL miRNA-specific primer (10 μL), 0.5 μ L mRQ 3′ primer, and 12.5 μ L SYBR Advantage Premix (2×). U6 was chosen as the PCR control. The datas were analyzed using $2^{-\Delta\Delta CT}$ method. Primer sequences used for qRT-PCR are listed in Supplementary Table I.

2.10. Statistical analysis

The original data were checked for normality and homogeneity of variance and are expressed as the means ± standard deviation (SD). Changes in age, gender, bone density (BMC, BMD, T score), BMI, serum biochemical Ca, Mg, P, and ALP levels, miRNAs PCR analyses, and statistical calculations were performed with SPSS 19.0 software (ver. 19.0; SPSS Inc., Chicago, IL, USA). When data were not normally distributed, a correction *t*'test was used. In all analyses, $P < 0.05$ was considered statistically significant. To analyze miRNA patterns in the control and GIOP groups, the miRNA counts were normalized using a modified global normalization method. Based on the normalized counts, the expression differences were measured by *t*-test. The EdgeR package (3.18.1) was used for differential expression analysis. miRNAs with a fold change ≥1.5 [up-regulated] or ≤1/1.5 (0.67) [down-regulated] and a *P*-value ≤ 0.05 were considered significant.

3. Results

3.1. General data baseline comparison

In the first discovery stage, there were two males and one female in the control group and one male and two females in the GIOP group. In the second verification stage, there were seven males and six females in the control group and six males and seven females in the GIOP group. There were no significant differences in age, BMI, serum P, serum ALP or serum Mg levels between the two groups, but serum Ca, BMC, BMD and T values were significantly lower in the GIOP group than in the control group ($P < 0.05$) (Tables 2 and 3).

3.2. RNA quality evaluation

The OD260/280 ratios of RNA were between 1.80 and 2.10, and the OD260/230 ratio exceeded 1.8 (Supplementary Table II); this suggested that the total RNA purity and quality were high. In addition, agarose gel electrophoresis (Supplementary Fig. 1) showed fairly sharp and intense bands at locations 28 s and 18 s, which indicated that the total RNA had good integrity was thus suitable for the construction of the sequencing library.

Table 2
General clinical data of two groups in the first discovery stage ($\bar{x} \pm s$).

Groups	Control group	GIOP group	T value	*P* value
Gender (male/female)	2/1	1/2	–	–
Age (year)	56.33 ± 7.37	57.67 ± 3.51	−0.283	0.791
BMI (kg/m^2)	20.31 ± 1.06	19.90 ± 1.84	0.333	0.756
BMC (g)	76.10 ± 8.03	30.26 ± 2.36	9.487	0.001
BMD (g/cm^2)	1.058 ± 0.062	0.538 ± 0.052	11.149	0.000
T value	−0.3 ± 0.5	−4.3 ± 0.2	11.537	0.000
Serum Ca (mmol/L)	2.39 ± 0.14	2.05 ± 0.05	3.881	0.012
Serum P (mmol/L)	1.14 ± 0.18	1.16 ± 0.76	0.645	0.554
Serum ALP (U/L)	85.67 ± 35.50	64.33 ± 26.08	0.682	0.533
Serum Mg (mmol/L)	0.89 ± 0.07	0.88 ± 0.03	0.079	0.941

Notes: "–" represents that this content is empty.

Table 3
General clinical data of two groups in the second verification stage ($\bar{x} \pm s$).

Groups	Control group	GIOP group	T value	P value
Gender (male/female)	7/6	6/7	–	–
Age (year)	56.40 ± 5.22	56.40 ± 4.92	0	1
BMI (kg/m^2)	21.02 ± 1.76	20.48 ± 1.72	0.483	0.642
BMC (g)	77.53 ± 6.02	31.92 ± 4.14	13.951	0.000
BMD (g/cm^2)	1.124 ± 0.102	0.552 ± 0.054	11.029	0.000
T value	−0.3 ± 0.9	−4.4 ± 0.1	10.702	0.000
Serum Ca (mmol/L)	2.37 ± 0.10	2.04 ± 0.05	6.126	0.000
Serum P (mmol/L)	1.25 ± 0.23	1.07 ± 0.07	1.651	0.180
Serum ALP (U/L)	78.60 ± 25.49	72.40 ± 21.84	0.413	0.690
Serum Mg (mmol/L)	0.89 ± 0.10	0.83 ± 0.10	0.819	0.437

Notes: "–" represents that this content is empty.

3.3. miRNA sequencing

All of the microRNA library molar concentrations in the two groups exceeded 1 fmol/L, with a fragment length of 130–155 nt, indicating that the constructed library was of high quality (Supplementary Table III). High quality clean reads were obtained by Illumina sequencing using Solexa CHASTITY, and the numbers of reads processed in each step are listed in Supplementary Table IV.

3.4. Differential miRNA expression analysis

In total, 374 miRNAs and 237 novel miRNAs were detected by next-generation sequencing (NGS) in the six samples. The top-10 TPMs values of the three GIOP and the three control groups were 147, 182, 148, 181, 166 and 165, respectively. Two miRNAs were significantly up-regulated, whereas seventeen known miRNAs and three novel miRNAs were significantly down-regulated. The differentially expressed miRNAs are shown in Table 4. Volcano and clustering plots of the differentially expressed miRNAs are shown in Fig. 1a and b. The chromosome locations of the differentially expressed miRNAs were also analyzed (horizontal lines on each chromosome represent a differentially expressed miRNA). The differentially expressed miRNAs were distributed on chromosomes 1, 3, 4, 5, 6, 7, 9, 11, 12, 17, 19, 22 and X (Supplementary Fig. 2).

3.5. Target gene prediction

Target gene prediction of the differentially expressed miRNAs was performed using TargetScan, miRanda and miRBase databases. Venn *diagram* was used to show the differentially expressed miRNA target genes. In total, 5983 targets were predicted in up-regulated miRNAs and 23,463 were predicted in down-regulated miRNAs. The number of predicted targets shared by hsa-miR-30c-2-3p and hsa-miR-214-5p in miRanda, miRBase and TargetScan database was 5,047, 1,344 and 0 of up-regulated miRNAs in miRanda, miRBase and TargetScan, respectively. No targets were common to all three databases, but 408 target genes were common to both miRanda and miRBase. There were 17,776, 6,239 and 4117 predicted targets in miRanda, miRBase and TargetScan database, respectively in down-regulated miRNAs, and 475 target genes were common to all three databases in down-regulated miRNAs (Fig. 2a and b).

3.6. Cytoscape network analysis

As shown in Fig. 3, Cytoscape networks were constructed to illustrate the relationships between miRNAs, miRNA-target genes in GIOP. For example, in the up-regulated miRNAs, the most enriched and crosslinked networks were the miR-214-5p and miR-30c-2-3p-target genes (Fig. 3a). In the down-regulated miRNAs, the most enriched and

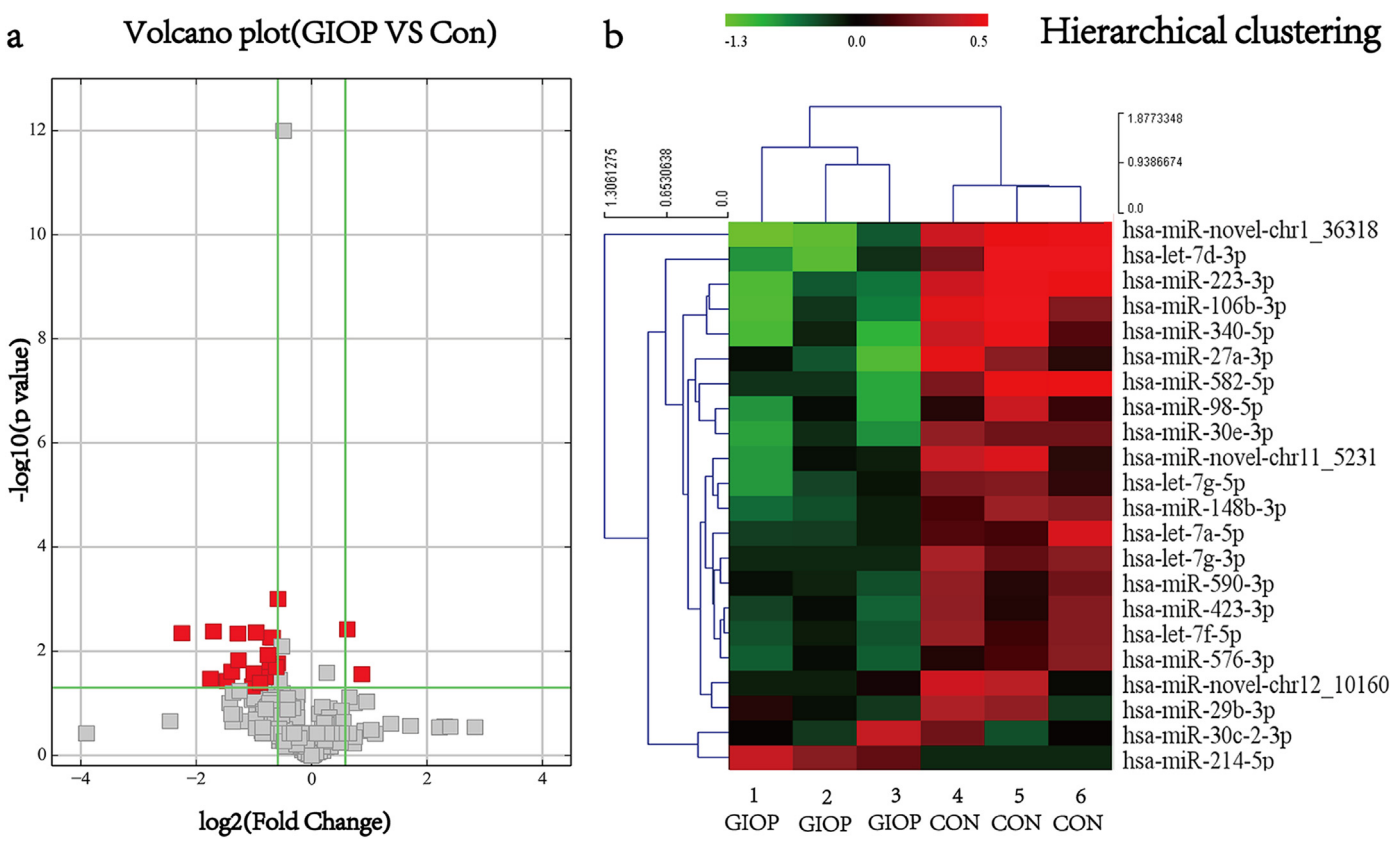

Fig. 1. Clustering of expression patterns of 22 differentially expressed miRNAs. The expression patterns of 22 differentially expressed miRNAs ($P < 0.05$) in the 6 patients libraries are displayed in the volcano plot and clustering plots. Volcano plot (a) and clustering (b) of miRNAs in the GIOP group and Control group (CON). (a) Volcano plot was constructed using *P*-values and fold-change of miRNAs, with log (*P*-value) as the ordinate and log2 (Fold change) for the abscissa. Red dots represent differentially expressed miRNAs between GIOP and Con Group ($P \leq 0.05$). (b) Hierarchical clustering was constructed according to the expression levels of miRNA, the six samples were classified into two groups. Green represents low relative expression, and red represents high relative expression. (For interpretation of the references to color in this figure legend, the reader is referred to the web version of this article.)

crosslinked networks were the miR-423-3p, miR-576-3p, miR-148-3p, let-7g-3p, let-7g-5p, let-7f-5p and let-7a-5p target genes (Fig. 3b).

3.7. Gene ontology (GO) analysis

GO enrichment analysis of differentially expressed miRNAs (DEMs) from GIOP revealed entries enriched in BP, CC, and MF. The target genes of these significantly altered miRNAs were enriched in 1939 GO

Table 4
Up-regulated and down-regulated miRNAs.

Mature ID	PRE-ID	Fold change	P value	Expression types	Sequence
hsa-miR-30c-2-3p	hsa-mir-30c-2	2.80	0.027	Up	CUGGGAGAAGGCUGUUUACUCU
hsa-miR-214-5p	hsa-mir-214	1.53	0.003	Up	UGCCUGUCUACACUUGCUGUGC
hsa-miR-423-3p	hsa-mir-423	0.66	0.016	Down	AGCTCGGTCTGAGGCCCCTCAGT
hsa-miR-576-3p	hsa-mir-576	0.65	0.019	Down	AAGATGTGGAAAAAT
hsa-miR-29b-3p	hsa-mir-29b	0.57	0.031	Down	TAGCACCATTTGAAATCAGTGTT
hsa-miR-590-3p	hsa-mir-590	0.50	0.026	Down	TAATTTTATGTATAAGCTAGT
hsa-miR-27a-3p	hsa-mir-27a	0.49	0.046	Down	TTCACAGTGGCTAAGTTCCGC
hsa-miR-582-5p	hsa-mir-582	0.41	0.014	Down	TTACAGTTGTTCAACCAGTTACT
hsa-let-7f-5p	hsa-let-7f	0.62	0.005	Down	TGAGGTAGTAGATTGTATAGTT
hsa-let-7a-5p	hsa-let-7a	0.63	0.028	Down	TGAGGTAGTAGGTTGTATAGTT
hsa-let-7d-3p	hsa-let-7d	0.29	0.033	Down	CTATACGACCTGCTGCCTTTCT
hsa-let-7g-5p	hsa-let-7g	0.66	0.001	Down	TGAGGTAGTAGTTTGTACAGTT
hsa-let-7g-3p	hsa-let-7g	0.60	0.020	Down	CTGTACAGGCCACTGCCTTGCT
hsa-miR-98-5p	hsa-mir-98	0.53	0.040	Down	TGAGGTAGTAAGTTGTATTGTT
hsa-miR-340-5p	hsa-mir-340	0.38	0.024	Down	TTATAAAGCAATGAGACTGATT
hsa-miR-223-3p	hsa-mir-223	0.30	0.004	Down	TGTCAGTTTGTCAAATACCCCA
hsa-miR-30e-3p	hsa-mir-30e	0.51	0.004	Down	CTTTCAGTCGGATGTTTACAGT
hsa-miR-148-3p	hsa-mir-148b	0.61	0.005	Down	TCAGTGCATCACAGAACTTTGT
hsa-miR-106b-3p	hsa-mir-106b	0.36	0.036	Down	TACCGCACTGTGGGTACTTGCT
hsa-miR-novel-chr12_10160	hsa-mir-novel-chr12_10160	0.59	0.011	Down	GCAUUGGUGGUUCAUUUG
hsa-miR-novel-chr11_5231	hsa-mir-novel-chr11_5231	0.41	0.004	Down	GCAGUGGUGGUCCAGUGG
hsa-miR-novel-chr1_36318	hsa-mir-novel-chr1_36318	0.41	0.004	Down	GCAUGAGUGGUUCAGUGG

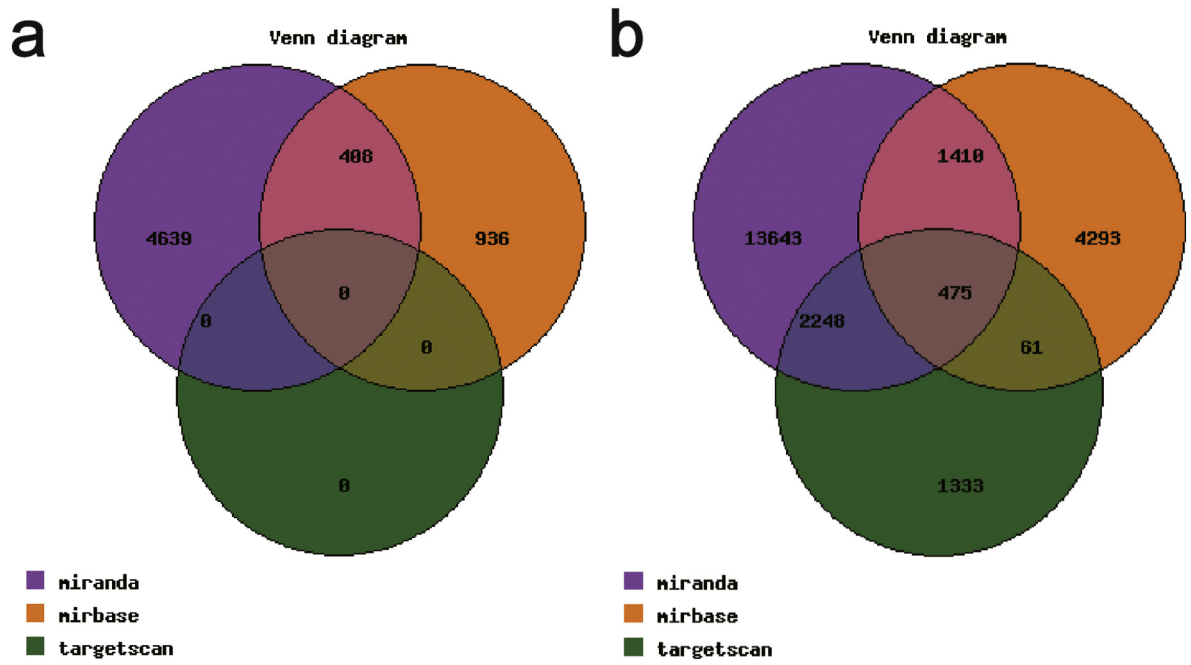

Fig. 2. Venn diagram of differentially expressed miRNA target genes. Venn diagram showed the expression distribution of all the target genes of differentially expressed miRNAs. Numbers in parentheses represents numbers of co-expressed or differentially expressed miRNAs. The Venn diagram of target genes in up-regulated miRNAs (a). The Venn diagram of target genes in down-regulated miRNAs (b). Target gene prediction of the differentially expressed miRNAs was performed using miRanda, miRBase and TargetScan databases.

terms. The top-10 GO terms are shown in Fig. 4. The up-regulated miRNAs were mainly enriched in actin filament-based process (GO:0030029, BP), anchoring junction (GO:0070161, CC), and cytoskeletal protein binding (GO:0008092, MF). The down-regulated miRNAs were enriched in multicellular organismal development (GO:0007275, BP), intracellular membrane-bounded organelle (GO:0043231, CC), and protein binding (GO:0005515, MF). Here, we listed the top-10 GO terms for up-regulated and down-regulated miRNAs based on the 3 ontologies (BP, CC and MF).

3.8. KEGG pathway analysis

KEGG pathway enrichment analysis revealed that the up- and down-miRNAs in the GIOP groups participate in 13 and 71 pathways, respectively. The top-10 signaling pathways of the up-regulated and down-regulated miRNAs are listed in Table 5 and Supplementary Fig. 3, respectively. Pathway analysis revealed that the most significantly enriched pathways associated with GIOP were the MAPK signaling pathway (pathway ID: hsa04010, Fig. 5), the FoxO signaling pathway (pathway ID: hsa04068, Fig. 6) and other metabolism-related pathways (e.g., Notch signaling pathway, pathway ID:hsa04330, Fig. 7) and the PI3K-Akt signaling pathway (pathway ID: hsa04151, Fig. 8). Furthermore, the target genes of hsa-miR-30c-2-3p, hsa-miR-214-5p, hsa-miR-576-3p, hsa-let-7a-5p, hsa-let-7f-5p, hsa-let-7g-5p, hsa-miR-148b-3p, hsa-miR-576-3p, and hsa-miR-423-3p showed significantly up- or down-regulated genes in the most significantly enriched pathways. A list of altered genes examined in MAPK, Notch, FoxO and PI3K-Akt signaling pathway and related miRNAs is shown in Table 6.

3.9. Novel miRNA prediction

A total of 237 novel miRNAs were found in the current study. However, according to the fold change status (≥ 1.5 [up-regulated] or ≤ 0.67 [down-regulated], $P < 0.05$), three down-regulated miRNAs were found, namely hsa-mir-novel-chr12_10160, hsa-mir-novel-chr11_5231 and hsa-mir-novel-chr1_36318. The predicted secondary structure maps of the novel miRNAs are shown in Fig. 9.

3.10. Verification of miRNAs by qRT-PCR

The qRT-PCR confirmed the sequencing results and indicated that hsa-miR-186-5p, hsa-miR-21-5p, hsa-miR-214-5p, hsa-miR-10b-5p, and hsa-miR-451a of the GIOP group were significantly up-regulated ($P < 0.05$), while, hsa-let-7f-5p, hsa-let-7a-5p, and hsa-miR-27a-3p were significantly down-regulated ($P < 0.05$, Fig. 10a and b). In addition, among the novel miRNAs, the expression of hsa-mir-novel-chr3_49413 was significantly up-regulated ($P = 0.005$). The secondary structure map of novel miR-novel-chr3_49413 is shown in Fig. 10c.

4. Discussion

The evidence of an important role of miRNAs in the regulation of bone remodeling continues to increase, and the association between miRNAs and bone loss disorders, such as osteoporosis, has been investigated by several group [13,29–33]. However, the role of miRNA expression in GIOP patients remains unclear.

Anastasilakis et al. [34] reported that the expression of miRNAs related to bone metabolism in the serum may be affected by anti-osteoporotic treatment; therefore, patients who accepted anti-osteoporotic treatment were excluded from the current study. Patients in the GIOP group had not received any anti-osteoporosis treatment.

In the current study, HTS and bioinformatics analysis revealed 19 miRNAs and 3 novel miRNAs that were differentially expressed in GIOP patients. However, only six significantly up-regulated miRNAs (including one up-regulated novel miRNA) and three significantly down-regulated miRNAs that may be closely associated with the molecular mechanism of GIOP were further verified.

hsa-miR-214-5p, hsa-miR-10b-5p, hsa-miR-21-5p, hsa-miR-451a, hsa-miR-186-5p, and hsa-miR-novel-chr3_49413, which are also closely associated with bone metabolism were significantly up-regulated in GIOP patients. miR214 inhibits the differentiation of osteoblasts and promotes the osteoclast differentiation by targeting ATF4, BIRC7, and FGFR1 to inhibit the PI3K/Akt, JNK and p38 pathways [35–39], while the inhibition of miR-214 promotes cell survival and extracellular matrix formation of osteoblastic MC3T3-E1 cells by targeting COL4A1

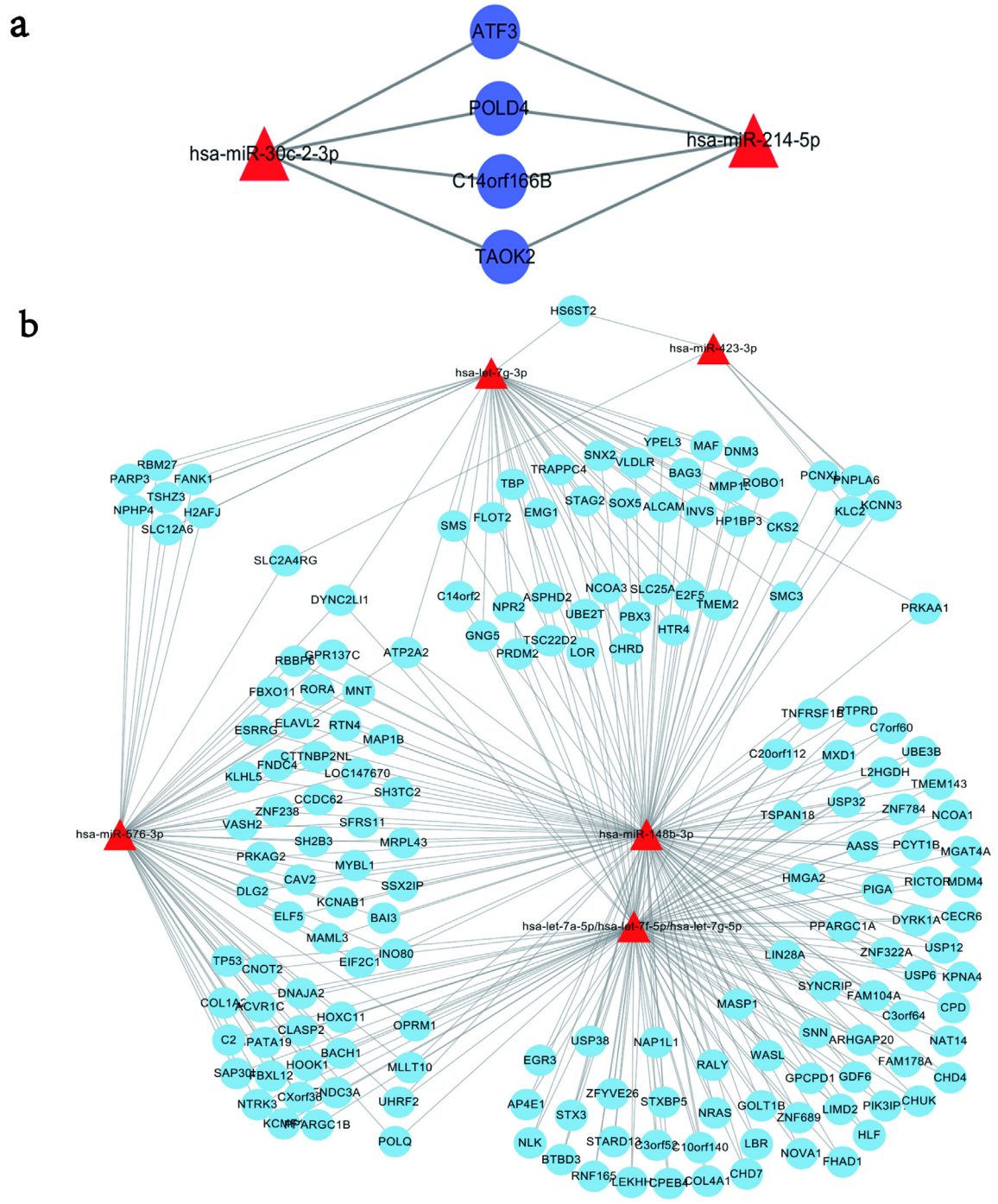

Fig. 3. A proposed network of putative interactions between miRNAs and mRNAs. Cytoscape networks were constructed to illustrate the regulation network of miRNAs and mRNAs involved in GIOP. Red triangles represent up- or down-regulated miRNAs, and blue or light green ellipses indicate the co-target genes. (a) miRNA-mRNA network among up-regulated miRNAs and their target mRNAs. ATF3, POLD4, C14orf166B and TAOK2 are the co-target genes of hsa-miR-214-5p and hsa-miR-30c-2-3p. (b) miRNA-mRNA network among down-regulated miRNAs and down-regulated mRNAs. hsa-miR-576-3p, has-let-7g-3p, has-miR423-3p, has-miR-148b, has-let-7f-5p and has-let-7g-5p have the common target genes. (For interpretation of the references to color in this figure legend, the reader is referred to the web version of this article.)

[40]. In addition, miR10b down-regulates the expression of E-cadherin, which plays an important role in the migration of bone marrow mesenchyme and stem cells in mice, and is weakly expressed during bone differentiation of induced pluripotent stem mouse cells induced by BMP4 [41,42]. The expression of miR21, which targets RECK, can improve osteoporosis [43]. However, the latest research also showed that a lack of miR21 inhibits bone differentiation and bone loss in mice, consistent with our results. Additionally, the expression of miR-21 was significantly higher in the serum of osteoporosis patients compared to control patients [44]. miR-451 also inhibits cell growth and invasion by targeting CXCL16, and its up- and down-regulation plays an essential role in fracture healing [45,46]. However, miR-186 was markedly reduced in the tibia of GIOP mice compared to controls in this study. This discrepancy may be due to differences in species or bone sampling site [47]. A novel miRNA (hsa-miR-novel-chr3_49413) was also significantly up-regulated in GIOP, but its structure and function remain

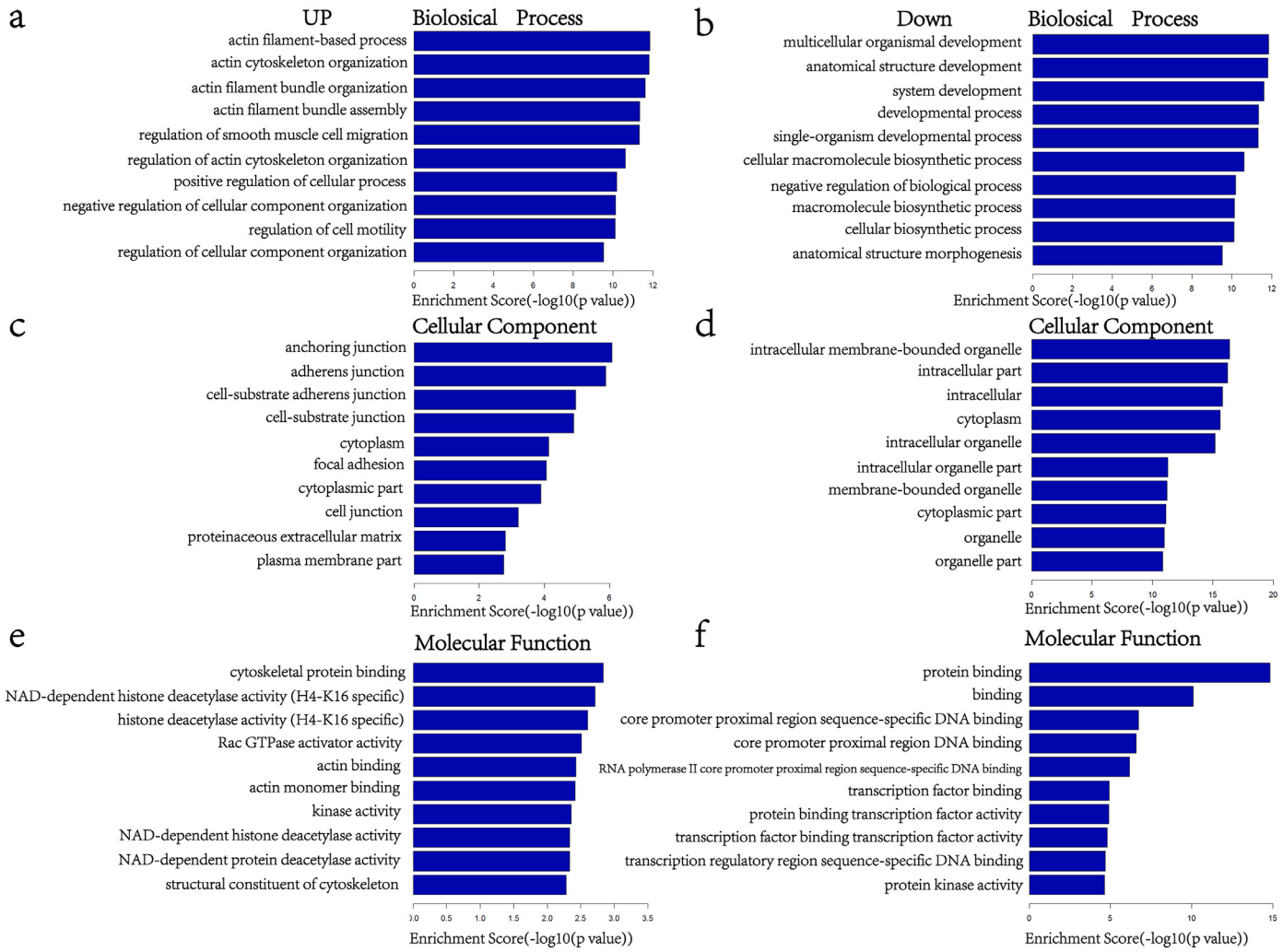

Fig. 4. GO terms for DEMs. GO enrichment score [− log 10(*P*-value)] analysis of up-regulated miRNAs and down-regulated miRNAs. Top-10 GO terms are showed.

elusive. Therefore, GIOP development may be closely associated with the up-regulation of the abovementioned miRNAs.

In contrast, hsa-let-7f-5p, hsa-let-7a-5p, and hsa-miR-27a-3p, which are related during the suppression of bone metabolism activity, were significantly down-regulated in GIOP. let-7f is crucial for the proliferation, metabolism activity and osteogenic differentiation capacity of human MSCs, by regulating the Wnt/β-catenin pathway via TIMP-1, and is markedly down-regulated in senescent stem cells [48,49]. let-7a has potential as a biomarker of osteogenic insufficiency. Conversely, up-regulation of let-7a could positively control the chondrogenic differentiation of mouse embryonic fibroblasts by targeting Chd4 [50,51]. A similar study revealed that miR-27a expression was significantly reduced in postmenopausal osteoporosis, confirming the role of miR-27a in bone formation [52]. miR27a demonstrably attenuated adipogenesis and promoted osteogenesis in steroid-induced rat bone marrow stem cells (BMSCs) by targeting PPARγ and GREM1, consistent with the reduction of GIOP observed in our study [53]. Therefore, the down-regulated miRNAs described in this study may regulate the genes involved in bone metabolism in GIOP. Taken together, the altered miRNAs verified by qRT-PCR provide important clues for further research.

Annotation of the biological functions of miRNAs, to predict their targets and construct regulation networks, is highly useful. Therefore, miRNA-mRNA network map construction, GO and pathway analyses were carried out to explore the regulatory mechanisms of miRNAs in GIOP. Through the integration of miRNA and mRNA expression data and miRNA-mRNA target prediction analysis, a number of putative miRNA-mRNA interactions were identified (Fig. 3). This study first performed GO enrichment analysis of vertebral samples of GIOP patients to reveal that the predicted target genes of altered miRNAs were significantly enriched in the down- and up-regulated GO terms, respectively; which was useful to fully describe BP, CC, and MF in relation to predicted target gene candidates.

Pathway analysis is the functional analysis of target genes in the KEGG pathway. A large number of miRNAs with diverse target genes aid understanding of essential BP in GIOP. In our study, top-10 pathway analysis showed that the differentially expressed miRNAs in GIOP were closely related to bone metabolism-related pathways such as FoxO, PI3K-Akt, MAPK and Notch signaling pathway (Table 6). A single miRNA has the potential to regulate multiple mRNAs, while multiple miRNAs can regulate a single mRNA; this enriches targets within a network or signaling pathway; therefore, miRNAs play key roles in diverse cellular processes and the pathogenesis of GIOP by regulating several pathways. For example, in our bioinformatics analysis, AKT2 (the common gene in down-regulated signaling pathways, such as the FoxO and PI3K-Akt signaling pathways) was the target gene of both hsa-let-7a-5p and hsa-let-7f-5p. hsa-let-7a-5p and hsa-let-7f-5p may regulate four related pathways by targeting AKT2 during the development of GIOP. Meanwhile, CCND1, IGF1 and IGF1R (common genes in the FoxO and PI3K-Akt signaling pathways), were the common target gene of hsa-let-7f-5p, which may regulate the three related pathways by targeting CCND1, IGF1 and IGF1R during the development of GIOP.

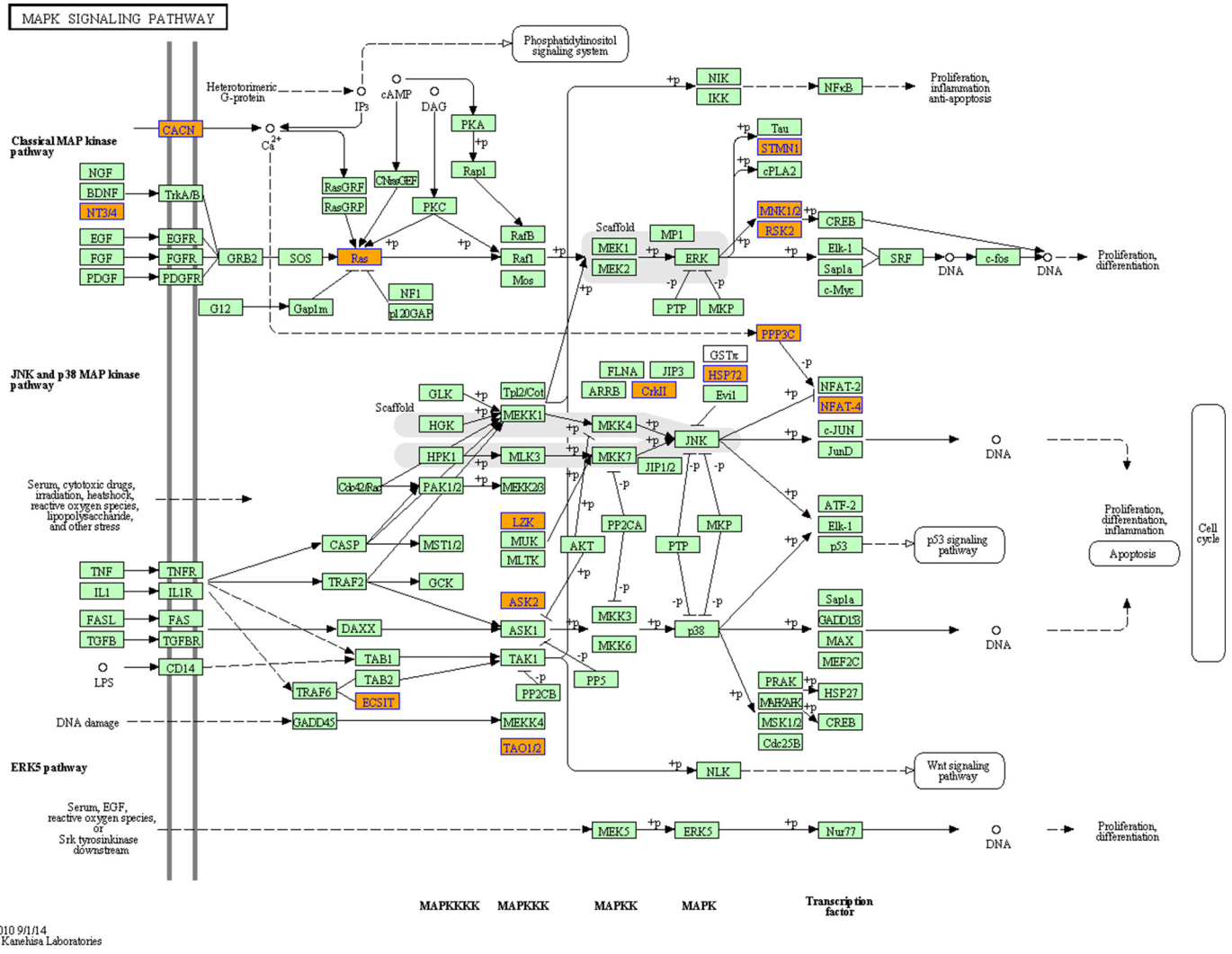

Fig. 5. The most significantly enriched pathways, up-regulated enriched pathway, MAPK signaling (pathway ID: hsa04010). The nodes with red frame and red symbol are associated with the DE genes. The DE genes associated with MAPK pathway are CACNA1E, CACNA1S, CACNG3, CRK, CRKL, ECSIT, HSPA2, MAP3K13, MAP3K6, MKNK2, MRAS, NFATC3, NTF3, PPP3R2, RPS6KA2, STMN1, and TAOK2. (For interpretation of the references to color in this figure legend, the reader is referred to the web version of this article.)

FoxO signaling regulates cellular physiological events including apoptosis and glucose metabolism, which is activated by of AMPK and JNK upon oxidative and nutrient stress stimuli and suppressed by Akt/PKB and PI3k in response to insulin or several growth factors, via exportation of FoxO proteins from the nucleus to the cytoplasm [54–58]. FoxOs attenuate bone formation by suppressing Wnt signaling. Conversely, recent studies have uncovered fundamental roles for FoxOs in skeletal homeostasis, and FoxO activation attenuates osteoclastogenesis via both cell autonomous and indirect mechanisms [59]. Additionally, FoxO proteins restrain osteoclastogenesis and bone resorption by attenuating H_2O_2 accumulation, and the deletion of FoxOs in osteoclasts decreases bone mass [60]. According to our study, GCs may suppress FoxO signaling by regulating hsa-miR-214-5p, hsa-miR-30c-2-3p, hsa-let-7a-5p, hsa-let-7f-5p, hsa-let-7g-5p, hsa-let-7g-3p, hsa-miR-148b-3p, hsa-miR-576-3p, and hsa-miR-423-3p.

The MAPK cascade, a highly conserved module, is involved in various cellular functions, including cell proliferation, differentiation and migration, and can be grouped by ERK-1/2, JNK1/2/3, p38 proteins, and ERK5 [61–65]. MAPK signaling plays a key role in osteogenesis and bone homeostasis [66–68]. The above results were consistent with bioinformatics data, in which MAPK was significantly down-regulated by the co-regulation of miRNAs (such as hsa-miR-214-5p, hsa-miR-30c-2-3p, hsa-let-7a-5p, hsa-let-7f-5p, hsa-let-7g-5p, has-let-7g-3p, hsa-miR-423-3p, and hsa-miR-148b-3p) in GIOP.

The PI3K-Akt signaling pathway, which is activated by many types of cellular stimuli and toxic insults, mainly regulates fundamental cellular functions [69]. Recent studies have demonstrated a close relationship between PI3K/Akt signaling and bone tissue metabolism [70,71]. The PI3K/Akt cell signaling pathway is involved in the inhibition of osteoporosis not only by promoting osteoblast proliferation and osteogenesis differentiation, but also by affecting osteoclast activity [36,70]. However, whether activation of the PI3K/Akt pathway is affected by miRNAs in GIOP remains unclear. The results from the present study indicate that the PI3K/Akt pathway is down-regulated by hsa-miR-214-5p, hsa-miR-30c-2-3p, hsa-let-7a-5p, hsa-let-7f-5p, hsa-let-7g-5p, hsa-let-7g-3p, hsa-miR-148b-3p, hsa-miR-576-3p, and hsa-miR-423-3p in GIOP.

The Notch signaling pathway is an evolutionarily conserved, intercellular signaling mechanism essential for proper embryonic development [72]. It is widely reported that Notch signaling could be a potential target for increasing bone formation in humans [73]. The preferential activation of Notch preferentially in osteocytes induces osteoprotegerin and Wnt signaling, thereby decreasing cancellous bone remodeling and increasing cortical bone formation [74]. Notch

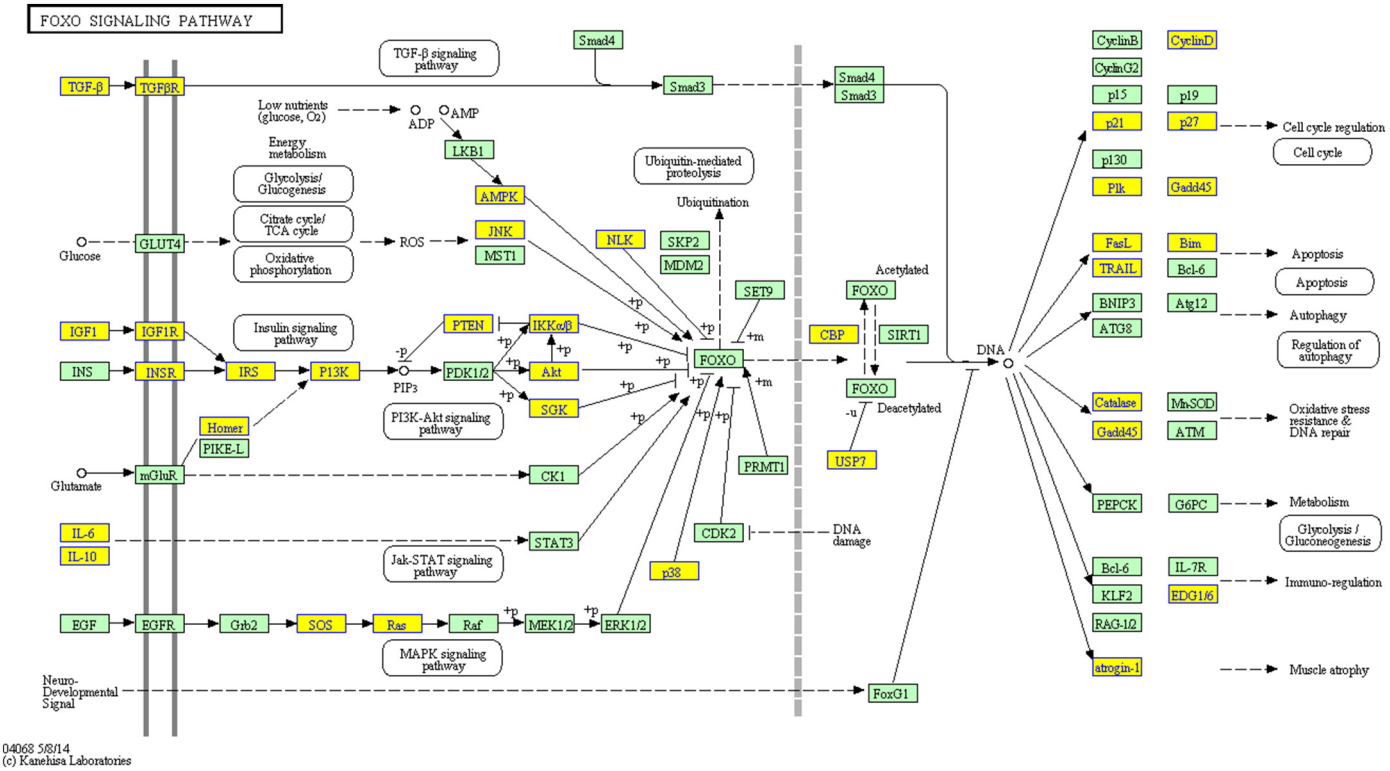

Fig. 6. The most significantly enriched pathways, down-regulated enriched pathway, FoxO signaling pathway (pathway ID: hsa04068). The nodes with yellow frame and yellow symbol are associated with the DE genes. The DE genes associated with FoxO pathway are AKT2, BCL2L11, CAT, CCND1, CDKN1A, CDKN1B, CHUK, CREBBP, EP300, FASLG, FBXO25, GADD45A, HOMER1, IGF1, IGF1R, IKBKB, IL10, IL6, INSR, IRS1, IRS2, MAPK11, MAPK9, NLK, NRAS, PIK3CA, PIK3CD, PIK3R3, PLK1, PRKAA1, PRKAB1, PRKAG2, PTEN, S1PR1, SGK1, SOS1, SOS2, TGFB2, TGFBR1, TNFSF10, and USP7. (For interpretation of the references to color in this figure legend, the reader is referred to the web version of this article.)

signaling enhances the proliferation and differentiation of human BMSCs, used to treat postmenopausal osteoporosis [75,76]. Notch signaling promotes the differentiation of preosteoblasts into osteoblasts but suppresses the differentiation of MSCs into pre-osteoblastic cells [74,77]. Our study presumed that GCs induced osteoporosis by down-regulating the Notch signaling pathway via hsa-miR-214-5, hsa-miR-30c-2-3p, hsa-let-7a-5p, hsa-let-7f-5p, hsa-let-7g-5p, hsa-let-7g-3p, and hsa-miR-576-3p.

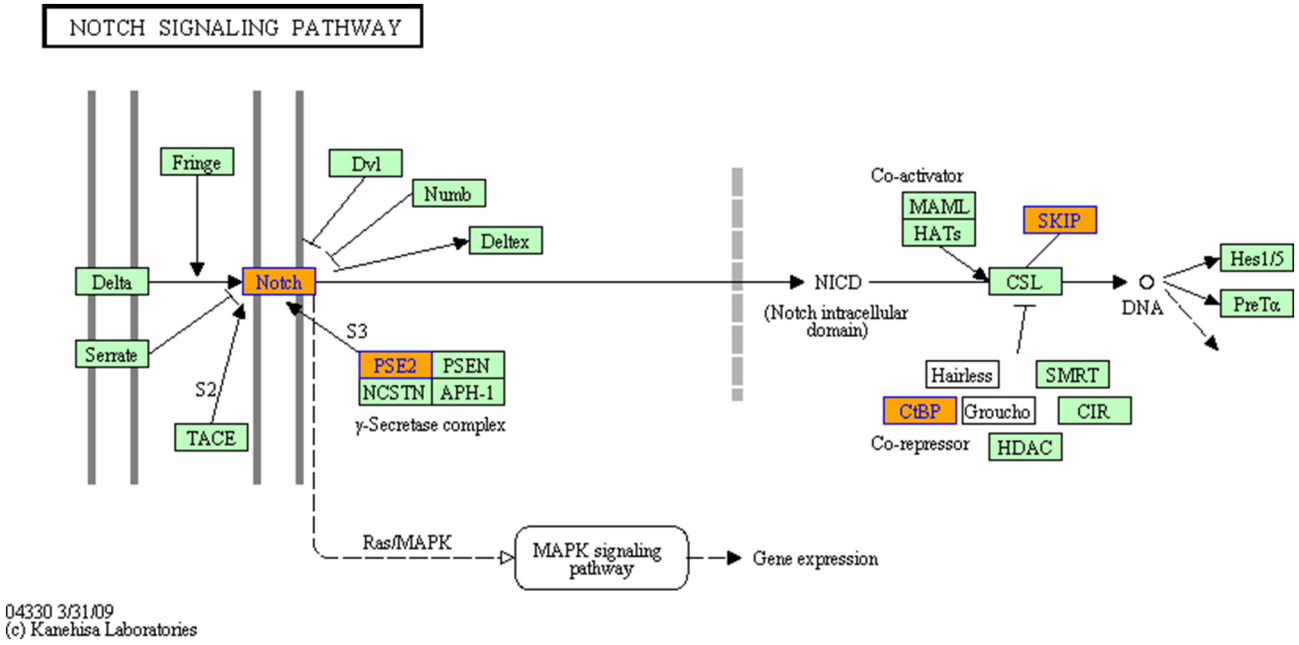

Fig. 7. The other up-regulated bone metabolism-related pathway (Notch signaling pathway, pathway ID: hsa04330). The nodes with red frame and red symbol are associated with the DE genes. The DE genes associated with Notch pathway are CTBP1, NOTCH4, PSENEN, and SNW1. (For interpretation of the references to color in this figure legend, the reader is referred to the web version of this article.)

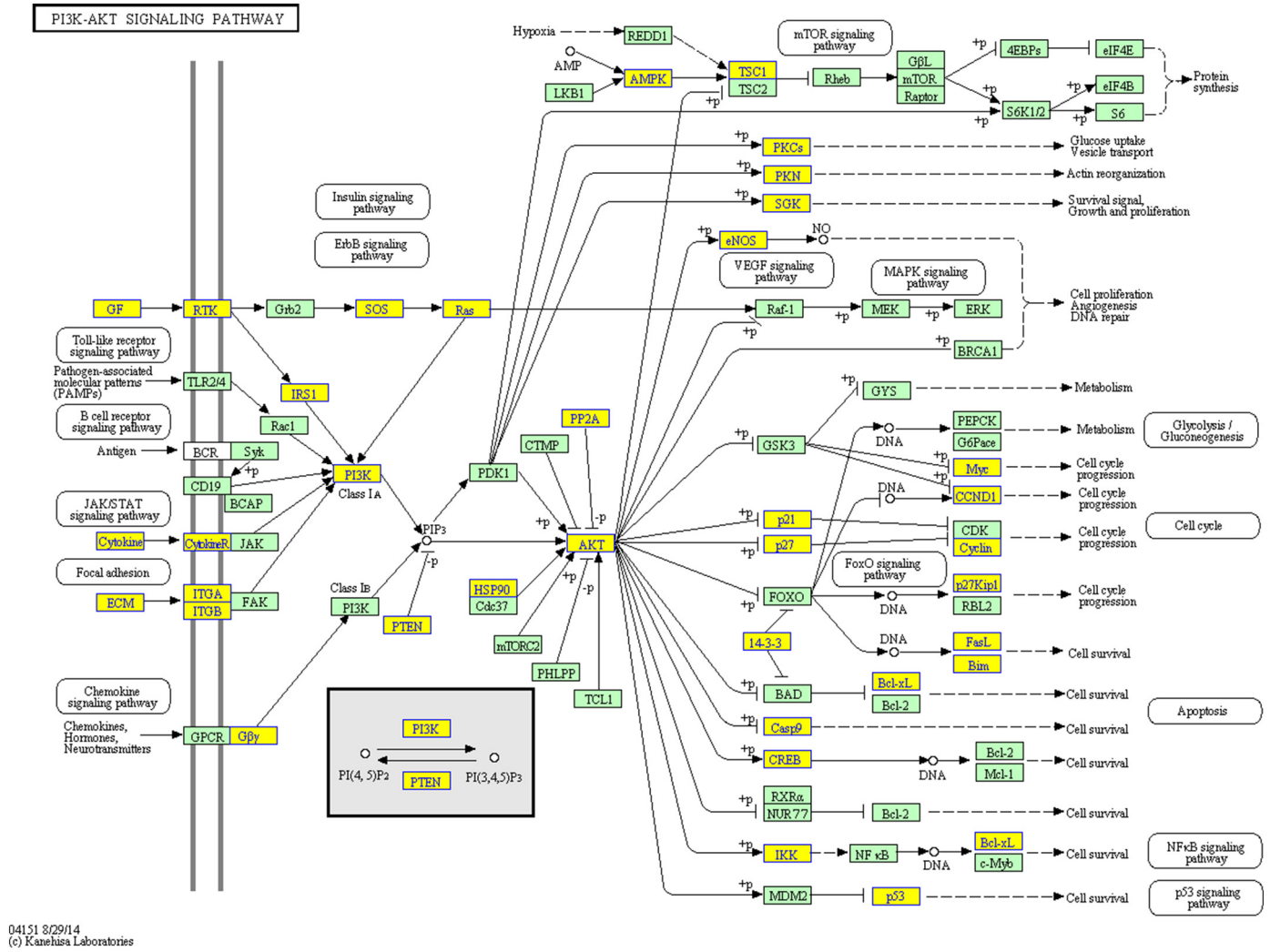

Fig. 8. The other down-regulated bone metabolism-related pathway (PI3K-Akt signaling pathway, pathway ID: hsa04151). The nodes with yellow frame and yellow symbol are associated with the DE genes. The DE genes associated with PI3K-Akt pathway are AKT2, BCL2L1, BCL2L11, CASP9, CCND1, CCNE2, CDKN1A, CDKN1B, CHUK, COL1A1, COL1A2, COL24A1, COL2A1, COL3A1, COL4A1, COL4A2, COL4A6, COL5A2, COL6A3, CREB3L1, CSF1, FASLG, FGF11, FGF2, FGFR2, FGFR4, GHR, GNB4, GNG5, HGF, HSP90B1, IGF1, IGF1R, IKBKB, IL2, IL6, INSR, IRS1, ITGA11, ITGA5, ITGA9, ITGB3, ITGB8, KIT, LAMA4, LAMB2, MET, MYC, NGF, NOS3, NRAS, OSM, OSMR, PDGFB, PIK3CA, PIK3CD, PIK3R3, PKN3, PPP2R5A, PPP2R5C, PPP2R5E, PRKAA1, PRKCZ, PTEN, SGK1, SOS1, SOS2, TEK, THBS1, TP53, TSC1, VEGFA, and YWHAB. (For interpretation of the references to color in this figure legend, the reader is referred to the web version of this article.)

5. Conclusion

Taken together, these results provide novel insight into the mechanism of GIOP. However, there were some limitations hardly avoided. For example, although relatively extensive sample size verification was carried out, the sample was still insufficient due to the limited time and funds. This study was also limited in terms of the gene screening that was performed. Moreover, a target gene was identified by the direction of change in a pairwise comparison, target prediction algorithms can result in a large number of false positive results. So, without any experimental data, one should be very careful applying these results. Therefore, we will further make use of in-vitro models of osteogenic differentiation, and perform animal studies using CRISPR/Cas9-mediated genome engineering to test whether modulation (up- or down-regulation) of the proposed GIOP microRNAs can in fact inhibit bone formation.

To the best of our knowledge, our study is one of the first to use vertebral samples of GIOP to perform miRNA-seq analysis and qRT-PCR validation. Using this strategy, we identified nine differentially expressed miRNAs finally; six miRNAs (hsa-miR-186-5p, hsa-miR-21-5p, hsa-miR-214-5p, hsa-miR-10b-5p, hsa-miR-451a, and hsa-miR-novel-chr3_49413) were significantly up-regulated and three (hsa-let-7f-5p, hsa-let-7a-5p, and hsa-miR-27a-3p) were significantly down-regulated. Thus, these miRNAs may be candidate regulatory genes for determining the mechanism of GIOP. To predict the biological function of the altered miRNAs, miRNA-mRNA network construction and GO term and related pathway analysis of the targets were performed. MAPK, FoxO, PI3K-Akt, and Notch signaling may act as regulatory pathways for anti-GIOP. In conclusion, our research provides further insight into the molecular mechanism of GIOP and lays a good foundation for the prevention and therapy of GIOP.

Supplementary data to this article can be found online at https://doi.org/10.1016/j.bone.2018.11.013.

Acknowledgements

This work was generously supported by the grants from project supported by GDUPS (2018), National Natural Science Foundation of China (81674000, 81774338, 81503591), Special Research Project for the Construction of the National TCM Clinical Research Base of the State Administration of Traditional Chinese Medicine (JDZX2015078), Excellent Young Scholars Project of China Association of Traditional

Table 5
KEGG pathways of differentially expressed miRNAs between GIOP and Control group patients' vatebral samples.

Pathway ID	Definition	Fisher-*P* value	FDR	Enrichment score
Up-regulated				
hsa04010	MAPK signaling pathway	0.000139265	0.04094389	3.856158
hsa05100	Bacterial invasion of epithelial cells	0.000535969	0.07878746	3.27086
hsa05410	Hypertrophic cardiomyopathy (HCM)	0.000814343	0.07980565	3.089192
hsa05414	Dilated cardiomyopathy	0.005800691	0.4263508	2.23652
hsa04260	Cardiac muscle contraction	0.01098459	0.6458938	1.959216
hsa04210	Apoptosis	0.01719555	0.8292558	1.764584
hsa05131	Shigellosis	0.01974419	0.8292558	1.704561
hsa04330	Notch signaling pathway	0.02779216	0.978869	1.556078
hsa05412	Arrhythmogenic right ventricular cardiomyopathy	0.03245282	0.978869	1.408748
hsa04360	Axon guidance	0.03329486	0.978869	1.477623
Down-regulated				
hsa04068	FoxO signaling pathway	2.48939E − 08	7.31882E-06	7.603906
hsa05215	Prostate cancer	6.55344E − 07	9.63356E-05	6.18353
hsa05205	Proteoglycans in cancer	1.74471E − 06	0.000170982	5.758276
hsa04151	PI3K-Akt signaling pathway	4.22608E − 06	0.000310617	5.374062
hsa05200	Pathways in cancer	9.02396E − 06	0.000530609	5.044603
hsa05214	Glioma	2.64305E − 05	0.001295096	4.577894
hsa05212	Pancreatic cancer	3.42413E − 05	0.001438134	4.46545
hsa04611	Platelet activation	5.63823E − 05	0.00207205	4.240857
hsa05222	Small cell lung cancer	0.000104704	0.003420321	3.980038
hsa05220	Chronic myeloid leukemia	0.000175189	0.005150559	3.756493

Note: “Pathway ID” stands for Pathway identifiers used in KEGG. “Definition” stands for the definition of the Pathway ID. “Fisher-*P* value” stands for the enrichment *P*-value of the Pathway ID used Fisher's exact test. “FDR” stands for the false discovery rate of the Pathway ID. “Enrichment_Score” stands for the Enrichment Score value of the Pathway ID, it equals “ − log10(*P* value)”.

Table 6
List of altered genes examined in MAPK, Notch, FoxO and PI3K-Akt pathway and related miRNAs.

Pathway	ID	Up/down	Selection counts	miRNA
MAPK	hsa04010	Up	CACNA1E, CACNA1S, CACNG3, CRK, CRKL, ECSIT, HSPA2, MAP3K13, MAP3K6, MKNK2, MRAS, NFATC3, NTF3, PPP3R2, RPS6KA2, STMN1, TAOK2	hsa-miR-214-5p hsa-miR-30c-2-3p hsa-let-7a-5p hsa-let-7g-5p hsa-let-7g-3p hsa-let-7f-5p hsa-miR-423-3p hsa-miR-148b-3p
Notch	hsa04330	Up	CTBP1, NOTCH4, PSENEN, SNW1	hsa-miR-214-5p hsa-miR-30c-2-3p hsa-let-7a-5p hsa-let-7f-5p hsa-let-7g-5p hsa-let-7g-3p hsa-miR-576-3p
FoxO	hsa04068	Down	AKT2, BCL2L11, CAT, CCND1, CDKN1A, CDKN1B, CHUK, CREBBP, EP300, FASLG, FBXO25, GADD45A, HOMER1, IGF1, IGF1R, IKBKB, IL10, IL6, INSR, IRS1, IRS2, MAPK11, MAPK9, NLK, NRAS, PIK3CA, PIK3CD, PIK3R3, PLK1, PRKAA1, PRKAB1, PRKAG2, PTEN, S1PR1, SGK1, SOS1, SOS2, TGFB2, TGFBR1, TNFSF10, USP7	hsa-miR-214-5p hsa-miR-30c-2-3p hsa-let-7a-5p hsa-let-7f-5p hsa-let-7g-5p hsa-let-7g-3p hsa-miR-148b-3p hsa-miR-576-3p hsa-miR-423-3p
PI3K-Akt	hsa04151	Down	AKT2, BCL2L1, BCL2L11, CASP9, CCND1, CCNE2, CDKN1A, CDKN1B, CHUK, COL1A1, COL1A2, COL24A1, COL2A1, COL3A1, COL4A1, COL4A2, COL4A6, COL5A2, COL6A3, CREB3L1, CSF1, FASLG, FGF11, FGF2, FGFR2, FGFR4, GHR, GNB4, GNG5, HGF, HSP90B1, IGF1, IGF1R, IKBKB, IL2, IL6, INSR, IRS1, ITGA11, ITGA5, ITGA9, ITGB3, ITGB8, KIT, LAMA4, LAMB2, MET, MYC, NGF, NOS3, NRAS, OSM, OSMR, PDGFB, PIK3CA, PIK3CD, PIK3R3, PKN3, PPP2R5A, PPP2R5C, PPP2R5E, PRKAA1, PRKCZ, PTEN, SGK1, SOS1, SOS2, TEK, THBS1, TP53, TSC1, VEGFA, YWHAB	hsa-miR-214-5p hsa-miR-30c-2-3p hsa-let-7a-5p hsa-let-7f-5p hsa-let-7g-5p hsa-let-7g-3p hsa-miR-148b-3p hsa-miR-576-3p hsa-miR-423-3p

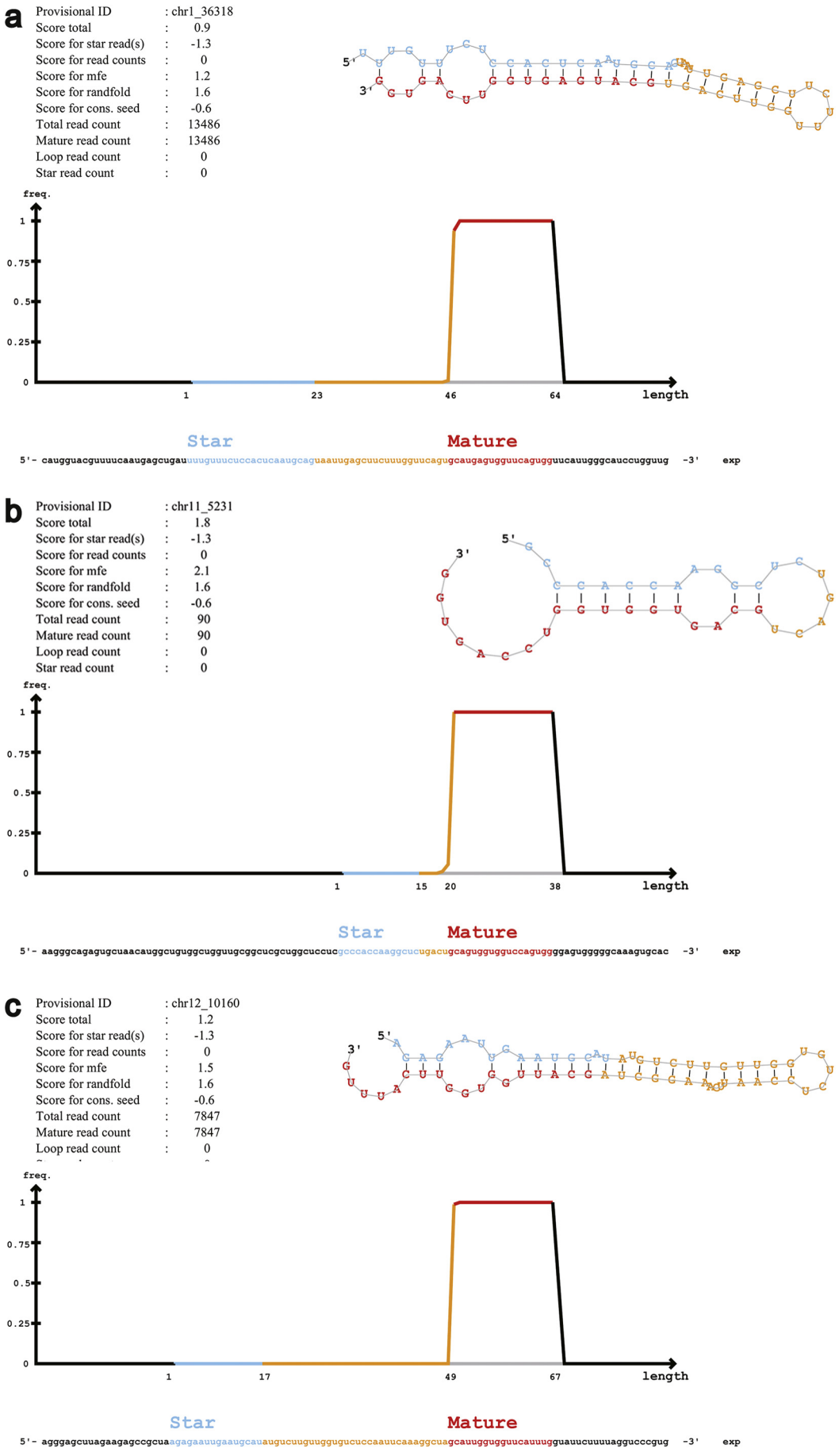

Fig. 9. Secondary structure of predicted pre-miRNA by miRDeep2. (a) hsa-miR-novel-chr1_36318, (b) hsa-miR-novel-chr11_5231, (c) hsa-miR-novel-chr12_10160.

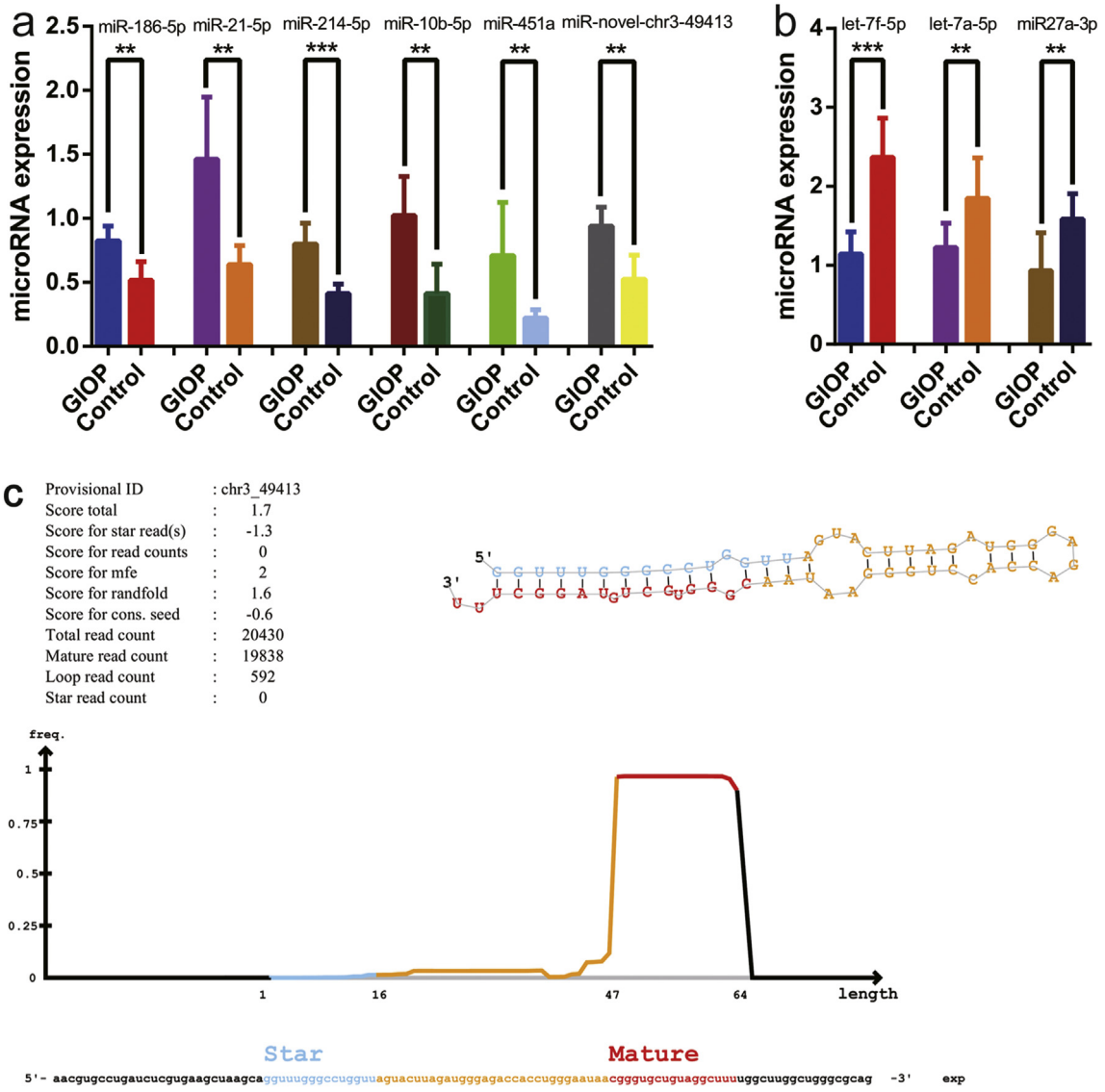

Fig. 10. Verification of microRNAs (miRNAs) by qRT-PCR. (a) Significantly up-regulated miRNAs, (b) Significantly down-regulated miRNAs, (c) The secondary structure map of novel miR-novel-chr3_49413. The results are expressed as the mean ± S.E.M. (three independent replicates per group). *$P < 0.05$, **$P < 0.01$, ***$P < 0.001$, N.S. = nonsignificant.

Chinese Medicine (CACM-2017-QNRC1-01), China Postdoctoral Science Foundation (2017M610271), Guangdong Science and Technology Department(2016A020226006, 2014A020221021), Natural Science Foundation of Guangdong Province(1614050002812, 2014A030310082), Science and Technology New Star of Guangzhou Pearl river (201710010078), Scientific Research Project of Traditional Chinese Medicine Bureau of Guangdong Province (20180330134046, 20161136), Excellent Doctoral Dissertation Incubation Grant of First Clinical School of Guangzhou University of Chinese Medicine (YB201602, YB201702), Excellent Young Scholars Project of the First Affiliated Hospital of Guangzhou University of Chinese Medicine (2015QN03, 2017QN08, 2017TD08).

Author contributions

All authors listed in the current study carried out the experiments, participated in the design of the study and performed the statistical analysis, conceived of the study, and helped to draft the manuscript. All authors read and approved the submitted manuscript.

Conflicts of interest

No potential conflicts of interest were disclosed.

References

[1] Y. Suzuki, Glucocorticoid-induced osteoporosis, Nihon Rinsho 73 (10) (2015) 1733–1739.
[2] R.M. Zebaze, A. Ghasem-Zadeh, A. Bohte, S. Iuliano-Burns, M. Mirams, R.I. Price, E.J. Mackie, E. Seeman, Intracortical remodelling and porosity in the distal radius and post-mortem femurs of women: a cross-sectional study, Lancet 375 (9727) (2010) 1729–1736, https://doi.org/10.1016/S0140-6736(10)60320-0.
[3] H. Ren, D. Liang, G. Shen, Z. Yao, X. Jiang, J. Tang, J. Cui, S. Lin, Effects of combined ovariectomy with dexamethasone on rat lumbar vertebrae, Menopause 23 (4) (2016) 441–450, https://doi.org/10.1097/GME.0000000000000547.
[4] G. Shen, H. Ren, T. Qiu, Q. Liang, J. Wei, Z. Tang, Z. Zhang, W. Yao, X.J. Zhao, Effect of glucocorticoid withdrawal on glucocorticoid inducing bone impairment, Biochem. Biophys. Res. Commun. 477 (4) (2016) 1059–1064, https://doi.org/10.1016/j.bbrc.2016.07.036.
[5] R. Rizzoli, Bone: towards a better management of glucocorticoid-induced osteoporosis? Nat. Rev. Rheumatol. 13 (11) (2017) 635–636, https://doi.org/10.1038/nrrheum.2017.141.
[6] J. Chou, P. Shahi, Z. Werb, microRNA-mediated regulation of the tumor microenvironment, Cell Cycle 12 (20) (2013) 3262–3271, https://doi.org/10.4161/cc.26087.

[7] L. He, G.J. Hannon, MicroRNAs: small RNAs with a big role in gene regulation, Nat. Rev. Genet. 5 (7) (2004) 522–531, https://doi.org/10.1038/nrg1379.
[8] B.N. Davis, A. Hata, Regulation of microRNA biogenesis: a miRiad of mechanisms, Cell Commun. Signal 7 (2009) 18.
[9] B.P. Lewis, C.B. Burge, D.P. Bartel, Conserved seed pairing, often flanked by adenosines, indicates that thousands of human genes are MicroRNA targets, Cell 120 (2005) 15–20.
[10] N. Laxman, C.-J. Rubin, H. Mallmin, et al., Second generation sequencing of microRNA in human bone cells treated with parathyroid hormone or dexamethasone, Bone 84 (2016) 181–188.
[11] L. Gennari, S. Bianciardi, D. Merlotti, MicroRNAs in bone diseases, Osteoporos. Int. 28 (4) (2017) 1191–1213, https://doi.org/10.1007/s00198-016-3847-5.
[12] J.B. Lian, G.S. Stein, A.J. van Wijnen, J.L. Stein, M.Q. Hassan, T. Gaur, Y. Zhang, MicroRNA control of bone formation and homeostasis, Nat. Rev. Endocrinol. 8 (4) (2012) 212–227, https://doi.org/10.1038/nrendo.2011.234.
[13] Y. Xie, L. Zhang, Y. Gao, W. Ge, P. Tang, The multiple roles of microrna-223 in regulating bone metabolism, Molecules 20 (10) (2015) 19433–19448, https://doi.org/10.3390/molecules201019433.
[14] B. Zuo, J. Zhu, J. Li, C. Wang, X. Zhao, G. Cai, Z. Li, J. Peng, P. Wang, C. Shen, Y. Huang, J. Xu, X. Zhang, X. Chen, microRNA-103a functions as a mechanosensitive microRNA to inhibit bone formation through targeting Runx2, J. Bone Miner. Res. 30 (2) (2015) 330–345, https://doi.org/10.1002/jbmr.2352.
[15] Z. Li, M.Q. Hassan, M. Jafferji, R.I. Aqeilan, R. Garzon, C.M. Croce, A.J. van Wijnen, J.L. Stein, G.S. Stein, J.B. Lian, Biological functions of miR-29b contribute to positive regulation of osteoblast differentiation, J. Biol. Chem. 284 (23) (2009) 15676–15684, https://doi.org/10.1074/jbc.M809787200.
[16] J. Zhang, Q. Tu, L.F. Bonewald, X. He, G. Stein, J. Lian, J. Chen, Effects of miR-335-5p in modulating osteogenic differentiation by specifically downregulating Wnt antagonist DKK1, J. Bone Miner. Res. 26 (8) (2011) 1953–1963, https://doi.org/10.1002/jbmr.377.
[17] T. Wang, Z. Xu, miR-27 promotes osteoblast differentiation by modulating Wnt signaling, Biochem. Biophys. Res. Commun. 402 (2) (2010) 186–189, https://doi.org/10.1016/j.bbrc.2010.08.031.
[18] M. Tome, P. Lopez-Romero, C. Albo, J.C. Sepulveda, B. Fernandez-Gutierrez, A. Dopazo, A. Bernad, M.A. Gonzalez, miR-335 orchestrates cell proliferation, migration and differentiation in human mesenchymal stem cells, Cell Death Differ. 18 (6) (2011) 985–995, https://doi.org/10.1038/cdd.2010.167.
[19] J.F. Zhang, W.M. Fu, M.L. He, W.D. Xie, Q. Lv, G. Wan, G. Li, H. Wang, G. Lu, X. Hu, S. Jiang, J.N. Li, M.C. Lin, Y.O. Zhang, H.F. Kung, MiRNA-20a promotes osteogenic differentiation of human mesenchymal stem cells by co-regulating BMP signaling, RNA Biol. 8 (5) (2011) 829–838, https://doi.org/10.4161/rna.8.5.16043.
[20] G. Li, J. Bu, Y. Zhu, X. Xiao, Z. Liang, R. Zhang, Curcumin improves bone microarchitecture in glucocorticoid-induced secondary osteoporosis mice through the activation of microRNA-365 via regulating MMP-9, Int. J. Clin. Exp. Pathol. 8 (12) (2015) 15684–15695.
[21] C. Shi, P. Huang, H. Kang, B. Hu, J. Qi, M. Jiang, H. Zhou, L. Guo, L. Deng, Glucocorticoid inhibits cell proliferation in differentiating osteoblasts by microRNA-199a targeting of WNT signaling, J. Mol. Endocrinol. 54 (3) (2015) 325–337, https://doi.org/10.1530/JME-14-0314.
[22] K. Liu, Y. Jing, W. Zhang, X. Fu, H. Zhao, X. Zhou, Y. Tao, H. Yang, Y. Zhang, K. Zen, C. Zhang, D. Li, Q. Shi, Silencing miR-106b accelerates osteogenesis of mesenchymal stem cells and rescues against glucocorticoid-induced osteoporosis by targeting BMP2, Bone 97 (2017) 130–138, https://doi.org/10.1016/j.bone.2017.01.014.
[23] X. He, W. Zhang, L. Liao, X. Fu, Q. Yu, Y. Jin, Identification and characterization of microRNAs by high through-put sequencing in mesenchymal stem cells and bone tissue from mice of age-related osteoporosis, PLoS One 8 (8) (2013) e71895, , https://doi.org/10.1371/journal.pone.0071895.
[24] X. Chen, Y. Ba, L. Ma, X. Cai, Y. Yin, K. Wang, J. Guo, Y. Zhang, J. Chen, X. Guo, Q. Li, X. Li, W. Wang, Y. Zhang, J. Wang, X. Jiang, Y. Xiang, C. Xu, P. Zheng, J. Zhang, R. Li, H. Zhang, X. Shang, T. Gong, G. Ning, J. Wang, K. Zen, J. Zhang, C.Y. Zhang, Characterization of microRNAs in serum: a novel class of biomarkers for diagnosis of cancer and other diseases, Cell Res. 18 (10) (2008) 997–1006, https://doi.org/10.1038/cr.2008.282.
[25] Y. Suzuki, On “2015 guidelines for prevention and treatment of osteoporosis”. Drug-induced osteoporosis: glucocorticoid-induced osteoporosis, Clin. Calcium 25 (9) (2015) 1347–1356 https://doi.org/CliCa150913471356.
[26] J.M. Grossman, R. Gordon, V.K. Ranganath, C. Deal, L. Caplan, W. Chen, J.R. Curtis, D.E. Furst, M. McMahon, N.M. Patkar, E. Volkmann, K.G. Saag, American College of Rheumatology 2010 recommendations for the prevention and treatment of glucocorticoid-induced osteoporosis, Arthritis Care Res. 62 (11) (2010) 1515–1526, https://doi.org/10.1002/acr.20295.
[27] G. Politano, A. Benso, A. Savino, S. Di Carlo, ReNE: a cytoscape plugin for regulatory network enhancement, PLoS One 9 (12) (2014) e115585, , https://doi.org/10.1371/journal.pone.0115585.
[28] M.R. Friedlander, S.D. Mackowiak, N. Li, W. Chen, N. Rajewsky, miRDeep2 accurately identifies known and hundreds of novel microRNA genes in seven animal clades, Nucleic Acids Res. 40 (1) (2012) 37–52, https://doi.org/10.1093/nar/gkr688.
[29] S. Zhu, F. Yao, H. Qiu, G. Zhang, H. Xu, J. Xu, Coupling factors and exosomal packaging microRNAs involved in the regulation of bone remodelling, Biol. Rev. Camb. Philos. Soc. 93 (1) (2018) 469–480, https://doi.org/10.1111/brv.12353.
[30] C.H. Hu, B.D. Sui, F.Y. Du, Y. Shuai, C.X. Zheng, P. Zhao, X.R. Yu, Y. Jin, miR-21 deficiency inhibits osteoclast function and prevents bone loss in mice, Sci. Rep. 7 (2017) 43191, , https://doi.org/10.1038/srep43191.
[31] S. Suttamanatwong, MicroRNAs in bone development and their diagnostic and therapeutic potentials in osteoporosis, Connect. Tissue Res. 58 (1) (2017) 90–102, https://doi.org/10.3109/03008207.2016.1139580.
[32] K. Gong, B. Qu, D. Liao, D. Liu, C. Wang, J. Zhou, X. Pan, MiR-132 regulates osteogenic differentiation via downregulating Sirtuin1 in a peroxisome proliferator-activated receptor beta/delta-dependent manner, Biochem. Biophys. Res. Commun. 478 (1) (2016) 260–267, https://doi.org/10.1016/j.bbrc.2016.07.057.
[33] X.H. Zhang, G.L. Geng, B. Su, C.P. Liang, F. Wang, J.C. Bao, MicroRNA-338-3p inhibits glucocorticoid-induced osteoclast formation through RANKL targeting, Genet. Mol. Res. 15 (3) (2016), https://doi.org/10.4238/gmr.15037674.
[34] A.D. Anastasilakis, P. Makras, M. Pikilidou, S. Tournis, K. Makris, I. Bisbinas, O. Tsave, J.G. Yovos, M.P. Yavropoulou, Changes of circulating microRNAs in response to treatment with teriparatide or denosumab in postmenopausal osteoporosis, J. Clin. Endocrinol. Metab. 103 (3) (2018) 1206–1213, https://doi.org/10.1210/jc.2017-02406.
[35] X. Wang, B. Guo, Q. Li, J. Peng, Z. Yang, A. Wang, D. Li, Z. Hou, K. Lv, G. Kan, H. Cao, H. Wu, J. Song, X. Pan, Q. Sun, S. Ling, Y. Li, M. Zhu, P. Zhang, S. Peng, X. Xie, T. Tang, A. Hong, Z. Bian, Y. Bai, A. Lu, Y. Li, F. He, G. Zhang, Y. Li, miR-214 targets ATF4 to inhibit bone formation, Nat. Med. 19 (1) (2013) 93–100, https://doi.org/10.1038/nm.3026.
[36] C. Zhao, W. Sun, P. Zhang, S. Ling, Y. Li, D. Zhao, J. Peng, A. Wang, Q. Li, J. Song, C. Wang, X. Xu, Z. Xu, G. Zhong, B. Han, Y.Z. Chang, Y. Li, miR-214 promotes osteoclastogenesis by targeting Pten/PI3k/Akt pathway, RNA Biol. 12 (3) (2015) 343–353, https://doi.org/10.1080/15476286.2015.1017205.
[37] L. Yang, D. Ge, X. Cao, Y. Ge, H. Chen, W. Wang, H. Zhang, MiR-214 attenuates osteogenic differentiation of mesenchymal stem cells via targeting FGFR1, Cell. Physiol. Biochem. 38 (2) (2016) 809–820, https://doi.org/10.1159/000443036.
[38] J. Liu, Y. Li, M. Luo, Z. Yuan, J. Liu, MicroRNA-214 inhibits the osteogenic differentiation of human osteoblasts through the direct regulation of baculoviral IAP repeat-containing 7, Exp. Cell Res. 351 (2) (2017) 157–162, https://doi.org/10.1016/j.yexcr.2017.01.006.
[39] Y.Z. Guo, L.H. Li, J. Gao, X.B. Chen, Q.H. Sang, miR-214 suppresses the osteogenic differentiation of bone marrow-derived mesenchymal stem cells and these effects are mediated through the inhibition of the JNK and p38 pathways, Int. J. Mol. Med. 39 (1) (2017) 71–80, https://doi.org/10.3892/ijmm.2016.2826.
[40] Q.S. Li, F.Y. Meng, Y.H. Zhao, C.L. Jin, J. Tian, X.J. Yi, Inhibition of microRNA-214-5p promotes cell survival and extracellular matrix formation by targeting collagen type IV alpha 1 in osteoblastic MC3T3-E1 cells, Bone Joint Res. 6 (8) (2017) 464–471, https://doi.org/10.1302/2046-3758.68.BJR-2016-0208.R2.
[41] F. Zhang, S. Jing, T. Ren, J. Lin, MicroRNA-10b promotes the migration of mouse bone marrow-derived mesenchymal stem cells and downregulates the expression of E-cadherin, Mol. Med. Rep. 8 (4) (2013) 1084–1088, https://doi.org/10.3892/mmr.2013.1615.
[42] H. Okamoto, Y. Matsumi, Y. Hoshikawa, K. Takubo, K. Ryoke, G. Shiota, Involvement of microRNAs in regulation of osteoblastic differentiation in mouse induced pluripotent stem cells, PLoS One 7 (8) (2012) e43800, , https://doi.org/10.1371/journal.pone.0043800.
[43] W. Zhao, Y. Dong, C. Wu, Y. Ma, Y. Jin, Y. Ji, MiR-21 overexpression improves osteoporosis by targeting RECK, Mol. Cell. Biochem. 405 (1–2) (2015) 125–133, https://doi.org/10.1007/s11010-015-2404-4.
[44] N. Yang, G. Wang, C. Hu, Y. Shi, L. Liao, S. Shi, Y. Cai, S. Cheng, X. Wang, Y. Liu, L. Tang, Y. Ding, Y. Jin, Tumor necrosis factor alpha suppresses the mesenchymal stem cell osteogenesis promoter miR-21 in estrogen deficiency-induced osteoporosis, J. Bone Miner. Res. 28 (3) (2013) 559–573, https://doi.org/10.1002/jbmr.1798.
[45] F. Zhang, W. Huang, M. Sheng, T. Liu, MiR-451 inhibits cell growth and invasion by targeting CXCL16 and is associated with prognosis of osteosarcoma patients, Tumour Biol. 36 (3) (2015) 2041–2048, https://doi.org/10.1007/s13277-014-2811-2.
[46] T. Waki, S.Y. Lee, T. Niikura, T. Iwakura, Y. Dogaki, E. Okumachi, K. Oe, R. Kuroda, M. Kurosaka, Profiling microRNA expression during fracture healing, BMC Musculoskelet. Disord. 17 (2016) 83, , https://doi.org/10.1186/s12891-016-0931-0.
[47] Y. Ma, H. Yang, J. Huang, Icariin ameliorates dexamethasone induced bone deterioration in an experimental mouse model via activation of microRNA186 inhibition of cathepsin K, Mol. Med. Rep. 17 (1) (2018) 1633–1641, https://doi.org/10.3892/mmr.2017.8065.
[48] J.M. Yu, X. Wu, J.M. Gimble, X. Guan, M.A. Freitas, B.A. Bunnell, Age-related changes in mesenchymal stem cells derived from rhesus macaque bone marrow, Aging Cell 10 (1) (2011) 66–79, https://doi.org/10.1111/j.1474-9726.2010.00646.x.
[49] V. Egea, S. Zahler, N. Rieth, P. Neth, T. Popp, K. Kehe, M. Jochum, C. Ries, Tissue inhibitor of metalloproteinase-1 (TIMP-1) regulates mesenchymal stem cells through let-7f microRNA and Wnt/beta-catenin signaling, Proc. Natl. Acad. Sci. U.S.A. 109 (6) (2012) E309–E316, https://doi.org/10.1073/pnas.1115083109.
[50] Z. Wang, Y. Lu, X. Zhang, X. Ren, Y. Wang, Z. Li, C. Xu, J. Han, Serum microRNA is a promising biomarker for osteogenesis imperfecta, Intractable Rare Dis. Res. 1 (2) (2012) 81–85, https://doi.org/10.5582/irdr.2012.v1.2.81.
[51] F. Sun, Q. Yang, W. Weng, Y. Zhang, Y. Yu, A. Hong, Y. Ji, Q. Pan, Chd4 and associated proteins function as corepressors of Sox9 expression during BMP-2-induced chondrogenesis, J. Bone Miner. Res. 28 (9) (2013) 1950–1961, https://doi.org/10.1002/jbmr.1932.
[52] L. You, L. Pan, L. Chen, W. Gu, J. Chen, MiR-27a is essential for the shift from osteogenic differentiation to adipogenic differentiation of mesenchymal stem cells in postmenopausal osteoporosis, Cell. Physiol. Biochem. 39 (1) (2016) 253–265, https://doi.org/10.1159/000445621.
[53] C. Gu, Y. Xu, S. Zhang, H. Guan, S. Song, X. Wang, Y. Wang, Y. Li, G. Zhao, miR-27a

attenuates adipogenesis and promotes osteogenesis in steroid-induced rat BMSCs by targeting PPARgamma and GREM1, Sci. Rep. 6 (2016) 38491, , https://doi.org/10.1038/srep38491.
[54] S.H. Ro, D. Liu, H. Yeo, J.H. Paik, FoxOs in neural stem cell fate decision, Arch. Biochem. Biophys. 534 (1–2) (2013) 55–63, https://doi.org/10.1016/j.abb.2012.07.017.
[55] X. Zhang, N. Tang, T.J. Hadden, A.K. Rishi, Akt, FoxO and regulation of apoptosis, Biochim. Biophys. Acta 1813 (11) (2011) 1978–1986, https://doi.org/10.1016/j.bbamcr.2011.03.010.
[56] K. Yamagata, H. Daitoku, Y. Takahashi, K. Namiki, K. Hisatake, K. Kako, H. Mukai, Y. Kasuya, A. Fukamizu, Arginine methylation of FOXO transcription factors inhibits their phosphorylation by Akt, Mol. Cell 32 (2) (2008) 221–231, https://doi.org/10.1016/j.molcel.2008.09.013.
[57] L.P. Van Der Heide, M.F. Hoekman, M.P. Smidt, The ins and outs of FoxO shuttling: mechanisms of FoxO translocation and transcriptional regulation, Biochem. J. 380 (Pt 2) (2004) 297–309, https://doi.org/10.1042/BJ20040167.
[58] L.O. Klotz, C. Sanchez-Ramos, I. Prieto-Arroyo, P. Urbanek, H. Steinbrenner, M. Monsalve, Redox regulation of FoxO transcription factors, Redox Biol. 6 (2015) 51–72, https://doi.org/10.1016/j.redox.2015.06.019.
[59] M. Almeida, Unraveling the role of FoxOs in bone—insights from mouse models, Bone 49 (3) (2011) 319–327, https://doi.org/10.1016/j.bone.2011.05.023.
[60] S.M. Bartell, H.N. Kim, E. Ambrogini, L. Han, S. Iyer, S. Serra Ucer, P. Rabinovitch, R.L. Jilka, R.S. Weinstein, H. Zhao, C.A. O'Brien, S.C. Manolagas, M. Almeida, FoxO proteins restrain osteoclastogenesis and bone resorption by attenuating H_2O_2 accumulation, Nat. Commun. 5 (2014) 3773, https://doi.org/10.1038/ncomms4773.
[61] S. Strack, T. Detzel, M. Wahl, B. Kuch, H.F. Krug, Cytotoxicity of TBBPA and effects on proliferation, cell cycle and MAPK pathways in mammalian cells, Chemosphere 67 (9) (2007) S405–S411, https://doi.org/10.1016/j.chemosphere.2006.05.136.
[62] W. Zhang, H.T. Liu, MAPK signal pathways in the regulation of cell proliferation in mammalian cells, Cell Res. 12 (1) (2002) 9–18, https://doi.org/10.1038/sj.cr.7290105.
[63] J. Kim, H. Lee, K.S. Kang, K.H. Chun, G.S. Hwang, Protective effect of Korean Red Ginseng against glucocorticoid-induced osteoporosis in vitro and in vivo, J. Ginseng Res. 39 (1) (2015) 46–53, https://doi.org/10.1016/j.jgr.2014.06.001.
[64] S.J. Harper, P. LoGrasso, Signalling for survival and death in neurones: the role of stress-activated kinases, JNK and p38, Cell. Signal. 13 (5) (2001) 299–310.
[65] K. Takeda, H. Ichijo, Neuronal p38 MAPK signalling: an emerging regulator of cell fate and function in the nervous system, Genes Cells 7 (11) (2002) 1099–1111.
[66] L.A. Stanton, F. Beier, Inhibition of p38 MAPK signaling in chondrocyte cultures results in enhanced osteogenic differentiation of perichondral cells, Exp. Cell Res. 313 (1) (2007) 146–155, https://doi.org/10.1016/j.yexcr.2006.09.027.
[67] W. Zhang, H. Guo, H. Jing, Y. Li, X. Wang, H. Zhang, L. Jiang, F. Ren, Lactoferrin stimulates osteoblast differentiation through PKA and p38 pathways independent of lactoferrin's receptor LRP1, J. Bone Miner. Res. 29 (5) (2014) 1232–1243.
[68] M. Liu, F. Fan, P. Shi, M. Tu, C. Yu, C. Yu, M. Du, Lactoferrin promotes MC3T3-E1 osteoblast cells proliferation via MAPK signaling pathways, Int. J. Biol. Macromol. 107 (Pt A) (2018) 137–143, https://doi.org/10.1016/j.ijbiomac.2017.08.151.
[69] M.A. Krasilnikov, hosphatidylinositol-3 kinase dependent pathways: the role in control of cell growth, survival, and malignant transformation, Biochemistry 65 (1) (2000) 59–67.
[70] J.C. Xi, H.Y. Zang, L.X. Guo, H.B. Xue, X.D. Liu, Y.B. Bai, Y.Z. Ma, The PI3K/AKT cell signaling pathway is involved in regulation of osteoporosis, J. Recept. Signal Transduct. Res. 35 (6) (2015) 640–645, https://doi.org/10.3109/10799893.2015.1041647.
[71] P.J. Marie, Signaling pathways affecting skeletal health, Curr. Osteoporos. Rep. 10 (3) (2012) 190–198, https://doi.org/10.1007/s11914-012-0109-0.
[72] C. Siebel, U. Lendahl, Notch signaling in development, tissue homeostasis, and disease, Physiol. Rev. 97 (4) (2017) 1235–1294, https://doi.org/10.1152/physrev.00005.2017.
[73] M.M. Roforth, K. Fujita, U.I. McGregor, S. Kirmani, L.K. McCready, J.M. Peterson, M.T. Drake, D.G. Monroe, S. Khosla, Effects of age on bone mRNA levels of sclerostin and other genes relevant to bone metabolism in humans, Bone 59 (2014) 1–6, https://doi.org/10.1016/j.bone.2013.10.019.
[74] E. Canalis, K. Parker, J.Q. Feng, S. Zanotti, Osteoblast lineage-specific effects of notch activation in the skeleton, Endocrinology 154 (2) (2013) 623–634, https://doi.org/10.1210/en.2012-1732.
[75] Y. Ji, Y. Ke, S. Gao, Intermittent activation of notch signaling promotes bone formation, Am. J. Transl. Res. 9 (6) (2017) 2933–2944.
[76] J.Z. Fan, L. Yang, G.L. Meng, Y.S. Lin, B.Y. Wei, J. Fan, H.M. Hu, Y.W. Liu, S. Chen, J.K. Zhang, Q.Z. He, Z.J. Luo, J. Liu, Estrogen improves the proliferation and differentiation of hBMSCs derived from postmenopausal osteoporosis through notch signaling pathway, Mol. Cell. Biochem. 392 (1–2) (2014) 85–93, https://doi.org/10.1007/s11010-014-2021-7.
[77] M.J. Hilton, X. Tu, X. Wu, S. Bai, H. Zhao, T. Kobayashi, H.M. Kronenberg, S.L. Teitelbaum, F.P. Ross, R. Kopan, F. Long, Notch signaling maintains bone marrow mesenchymal progenitors by suppressing osteoblast differentiation, Nat. Med. 14 (3) (2008) 306–314, https://doi.org/10.1038/nm1716.